

## 2.2 OSIRIS CHAMBER DESIGN AND ANALYSIS

### 2.2.1 Evolution of Design

#### 2.2.1.1 Design Goals

The primary goal of the Osiris concept is to devise a low activation chamber design that is innovative, but requires no great leaps in technology. Other goals are leak tolerance, low pressure operation, low tritium inventory, rapid changeout of neutron-damaged parts, low vapor density in the chamber, and high power conversion efficiency.

#### 2.2.1.2 Earlier Concepts

**First Version.** Figure 2.2 shows the first embodiment of Osiris. There are two pools of liquid coolant (originally lithium-lead), one each above and below the target chamber. The coolant flows by gravity through an annular carbon fabric "sock" from one pool to the other. It also weeps to the surface of the first wall, providing a sacrificial film that protects the fabric from damaging x-ray and debris energy from the target. The similarities to the HYLIFE<sup>2.1</sup> and HIBALL<sup>2.2</sup> designs are readily apparent. The primary advantages over HYLIFE are the greater control of flow rate and the reduced impact of isochoric heating.

The system is very leak tolerant with everything dropping to the lower pool. At changeout time, the liquid is completely drained to the lower pool, and the empty carbon sock is lifted out the top.

The key issue that arose from this design centered around heat removal. Most of the vaporized coolant was expected to condense on the first wall; a smaller fraction condensed in the pool. Because heat fluxes were so high, a great deal of coolant turbulence was needed to prevent overheating, which would ultimately create excess vapor in the chamber which would interfere with HIB propagation.

**Second Version.** The next version, shown in Fig. 2.3, attempted to solve the heat flux problem by using baffles placed at a shallow angle to the target. In addition to providing a large surface area, the back side of the baffles could be used for vapor condensation. The baffles would also shield the rear blankets, which would receive neutron heating only.

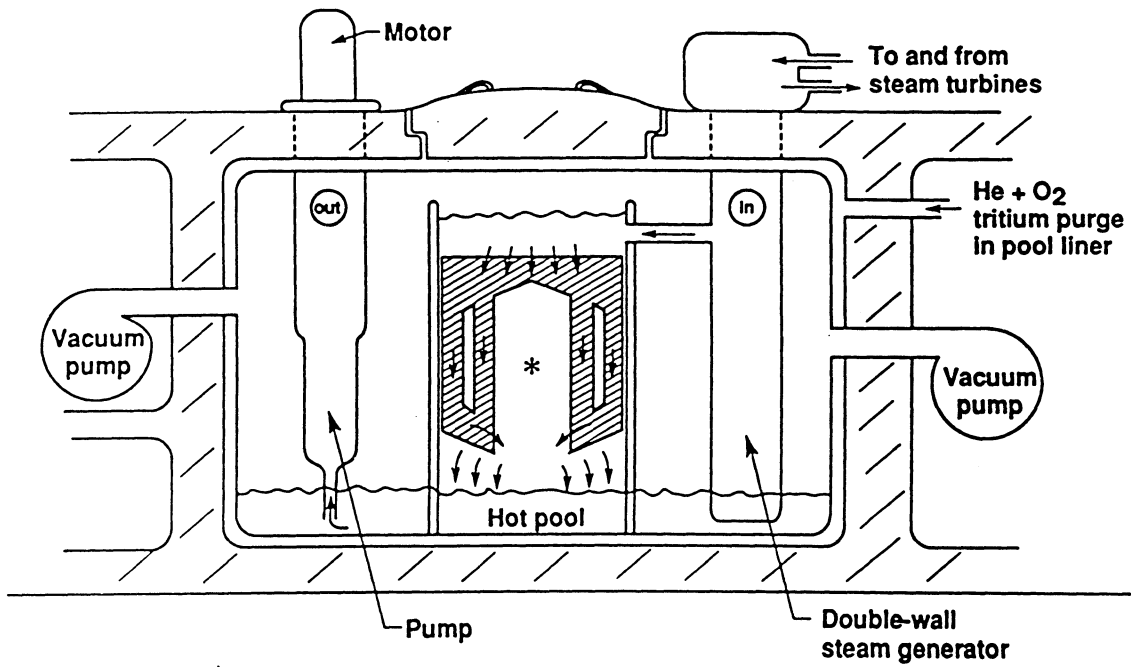


Fig. 2.2. The original version of Osiris using lithium lead.

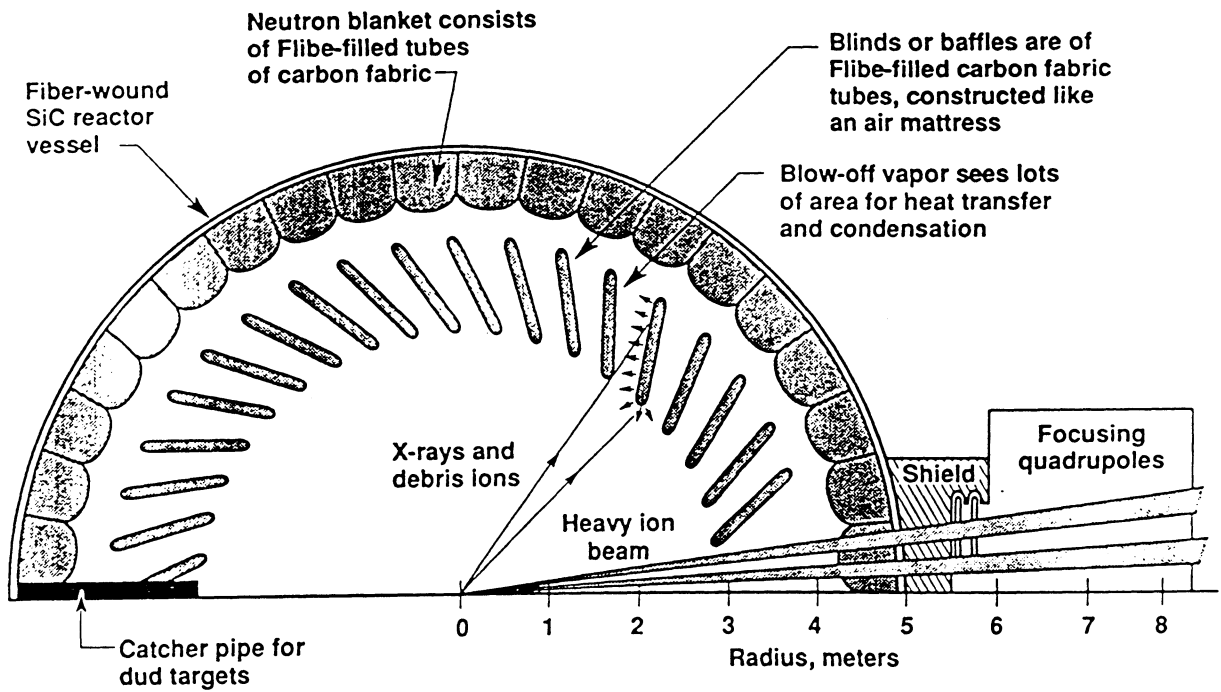
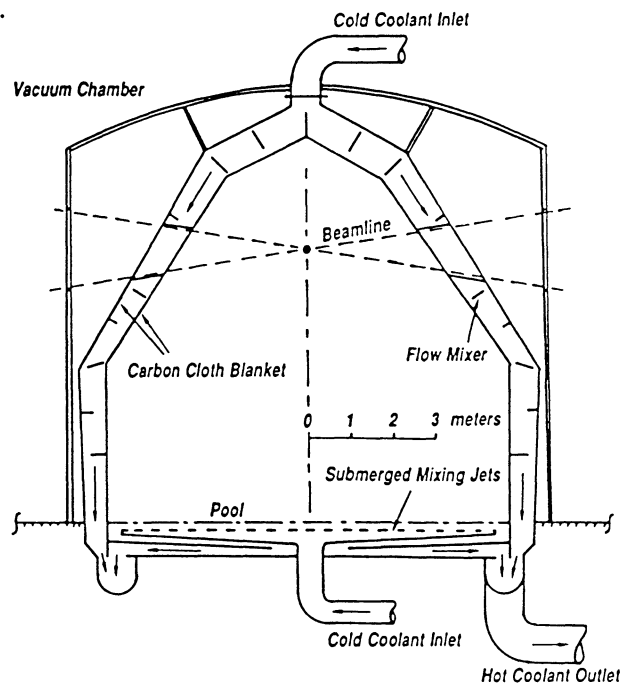


Fig. 2.3. The second version of Osiris using Flibe. The thin panels are intended to compensate for the poor thermal conductivity of Flibe.

Because the baffles were fairly thin, impulse loading created structural problems that were difficult to assess. Also, while the heat flux issue was largely resolved over most of the surface area, the curved sides of the baffles nearest the target still received the full impact. Lastly, while the concept resolved some problems for the chamber walls, the issue of the chamber roof was left unresolved.

**Third Version.** A fundamental design change occurred in the next version, shown in Fig. 2.4. Rather than attempt to condense the blowoff vapor back on the wall, it was directed toward the pool where it was condensed. This greatly relieved the heat flux and overheating problems on the wall, which became especially serious when the blanket coolant was switched from LiPb to the lower activation, but poorly conducting, Flibe (2 LiF + BeF<sub>2</sub> molten salt). In this version, the blanket took on a tepee-like shape, and the angled panels were eliminated. With this geometry, the blowoff vapor was directed downward toward the pool. The pool was far enough from the target that it did not generate a counterflow blowoff vapor. A perforated plate in the pool generated jets that churned the surface, creating enough turbulence to condense the vapor. With the exception of energy radiated to the first wall by the hot vapor, little heat transfer took place along the wall. The primary heat transfer for condensation was by direct contact of the vapor with the pool.



**Fig. 2.4.** The third version of Osiris where the Flibe vapor condenses in the pool rather than on the first wall.

### 2.2.1.3 Final Design

The final design evolved from the third design to the one shown in Fig. 2.5. It retains the essential elements of the previous version with small but significant changes. The pool is closer to the target reducing the height of the chamber and volume of blanket, but the pool contribution to blowoff vapor remains small. It was not that necessary to direct the blowoff toward the pool. Even a quiescent gas filling the volume will condense quickly if the pool can absorb the heat without overheating. The perforated plates in the pool are replaced with spray nozzles around the blanket. (The plates, being closer now to the target, would have had to be replaced periodically.) The nozzles are shielded from direct exposure to fusion neutrons.

The coolant now makes two passes through the blanket. The first is at high speed, and the temperature rise is only 20°C. The coolant then makes a U-turn and goes up the outer channel collecting the bulk of the neutron heat. It then tumbles down the outside of the blanket, releasing some of the bred tritium to the vacuum system. At the bottom of the reactor, the coolant dumps into an annular blanket and mixes with the pool flow at the exit.

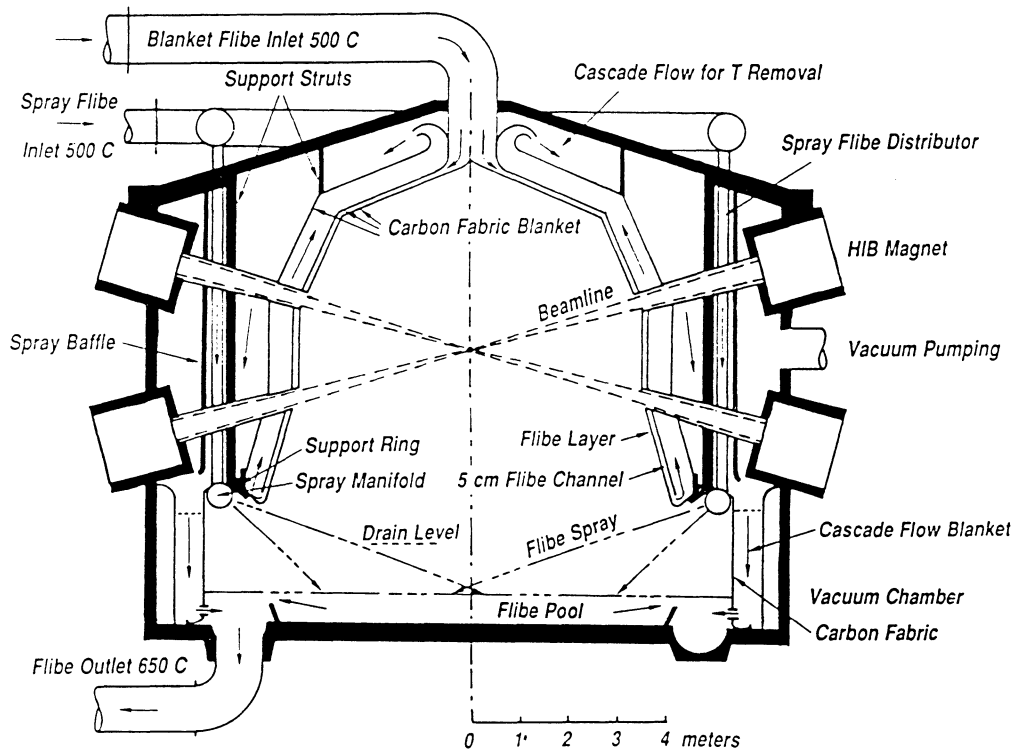


Fig. 2.5. The final version of Osiris with sprays to ensure vapor condensation. Shown for two-sided illumination using final beam geometry.

This arrangement is fairly simple to implement and assures a low vapor temperature in the chamber. The design reflects an improved understanding of the vaporization process. The Flibe coating on the first wall boils off down to a depth and temperature where the boiling point of the Flibe corresponds to the vapor pressure in the chamber. The temperature distribution in the Flibe, which is created by the X-ray deposition from the target, must at some point fall below this boiling point, or the Flibe will be a continuous source of vapor. By providing a high-speed, low-temperature flow channel behind the first wall, the temperature distribution of the Flibe coating the first wall is controlled and the layer boiled off is very thin. A Flibe vapor density of about  $5 \cdot 10^{18} \text{ m}^{-3}$  will strip an extra electron each from about 30% of the ions in the beam over a 5 m propagation distance (see Section 2.4). This amount of stripping has little effect on the beam spot size. This Flibe density corresponds to a temperature of  $570^\circ\text{C}$ . The bulk Flibe temperature near the wall must be kept below this limit. To allow some margin, the Flibe enters at  $500^\circ\text{C}$ ,  $40^\circ$  above the melting point, and leaves the first wall region at  $520^\circ\text{C}$ . While the spray does heat up to  $607^\circ\text{C}$ , the average in transit is  $554^\circ\text{C}$ , so excess vapor generation should not occur.

## **2.2.2 First Wall Protection**

Because ballistic focusing of heavy ion beams requires a low chamber fill gas density (we have allowed a number density of  $5 \times 10^{18} \text{ molecules m}^{-3}$ ) and limited focusing distances, the first wall of the reactor is exposed to high intensities of x-ray radiation from the target. As discussed above, we protect the first wall fabric with continuous coating of liquid Flibe. Vaporized Flibe is replaced by liquid Flibe seeping through the woven graphite that supports the film. This section examines the vaporization process and the resulting stresses on the first wall.

### **2.2.2.1 Target Emanations**

The Osiris targets emit x-rays, neutrons, and ions. The assumed target parameters are given in Table 2.2. The calculations presented in this section were based on a preliminary estimate for the target gain. The assumed target gain was increased by 18% as the driver design improved, so the results presented here should be scaled with target yield.

The interaction between target emissions and reactor gases and surfaces is dependent upon the spectra and timing of the target radiation. The x-ray spectrum assumed in this study was

taken from the HIBALL-II report.<sup>2,3</sup> The target debris ion species and energies used in these calculations are given in Table 2.3.

**Table 2.2. Target Parameters for Osiris**

	Assumed	Base Case
Energy on Target (MJ)	5	5
Target Gain	73	86.5
Target Yield (MJ)	365	432
Neutron Yield (MJ)	256	303
X-ray and Debris Yield (MJ)	109	129

**Table 2.3. Target Debris Ion Energies**

Normalized Energy (keV/amu)	0.85
Deuterium Energy (keV)	1.70
Tritium Energy (keV)	2.55
Helium-4 (keV)	3.40
Lithium-7 (keV)	5.90
Lead 207 (keV)	176.0

#### 2.2.2.2 CONRAD Computer Code

The CONRAD<sup>2,4</sup> computer code was used to analyze reactor chamber designs for Osiris. CONRAD is a one-dimensional Lagrangian finite difference computer code that calculates hydrodynamic motion, radiation transport, and vaporization and condensation in planar, cylindrical, or spherical geometries. Radiation transport is calculated with flux limited multi-

group diffusion. Time dependent target x-ray and ion deposition are calculated in the fill gas and walls. Heat transfer calculations are performed by CONRAD to get wall surface temperatures and temperature profiles in the wall at all times. These temperature profiles are used to calculate vaporization and condensation rates.

Equation-of-state and opacity data are read by CONRAD from tables. The properties of the materials are assumed to be quasi-static. The data tables are created with equation-of-state results from the IONMIX<sup>2.5</sup> computer code or from the SESAME<sup>2.6</sup> library. IONMIX is better suited to materials much less dense than solids or liquids, while SESAME is preferred at higher densities. Opacity tables are constructed with results from IONMIX. Twenty energy group opacities are used in these calculations.

CONRAD calculates the amount of material vaporized by the target x-rays when the x-rays volumetrically heat the absorbing material to above the energy required to vaporize the material. The x-rays arrive at the material in a pulse applying a time-dependent power to the surface. The x-rays are divided into photon energy groups, and each group has a separately calculated deposition length in the material. An example deposition profile in the material is shown in Fig. 2.6. The energy density profiles are time-dependent since the x-ray fluence is spread over a finite pulse width and because heat is conducted away from the heated inner surfaces.

Figure 2.6 illustrates how the thickness of the vaporized material is calculated; the vaporization energy density and sensible heat at the vaporization temperature are shown. The vaporization temperature is calculated as a function of the local vapor pressure. Three regions are defined in the material. Region A is where material gains an energy density above that required for vaporization and is vaporized. In Region C, the material remains below the sensible heat of the material, and none of the material is vaporized. Because the material in Region B gains energy beyond the sensible energy but below the vaporization energy, the extent of vaporization in Region B is uncertain. We have estimated vaporization in Region B by using the total energy deposited in the region and calculating the corresponding amount of material that could be raised to its vaporization energy; this amount of material is assumed to be vaporized.

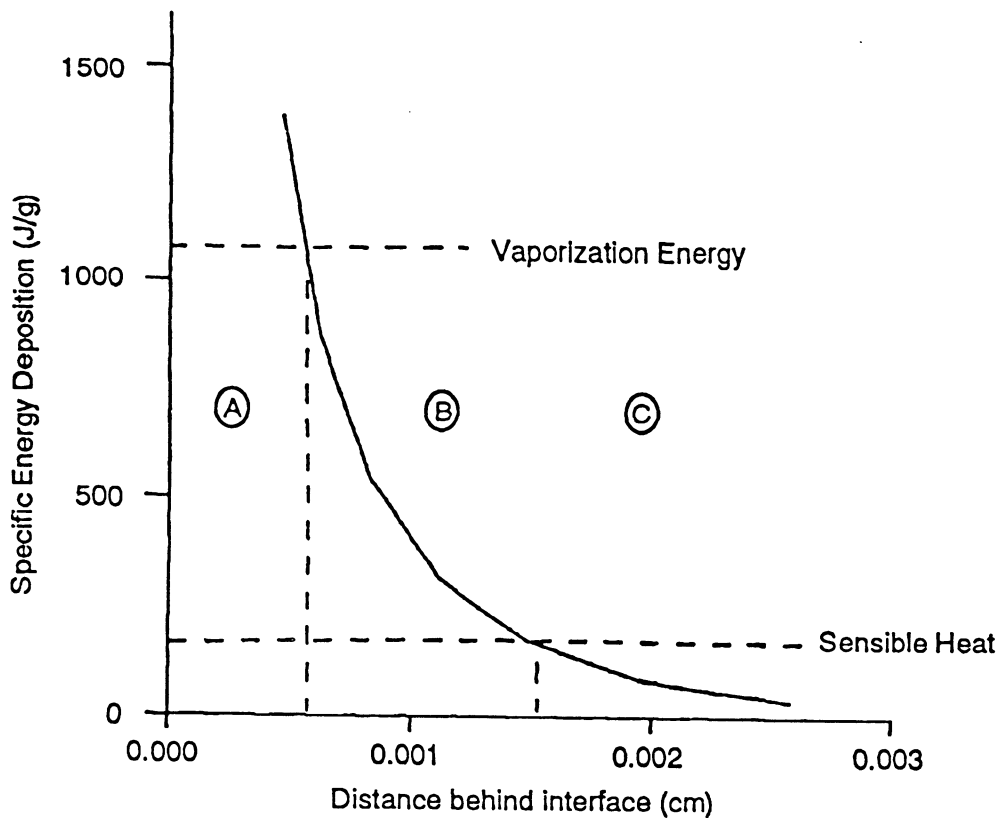


Fig. 2.6. Sample time-dependent energy profile from deposited X-rays.

### 2.2.2.3 Vaporization

A CONRAD simulation for Osiris was performed using a yield of 365 MJ. The essential calculated parameters for Osiris are given in Table 2.4. These results are proportional to the target yield for yields within 20% of the 365 MJ assumed yield. The results for the base case yield of 432 MJ are also shown. The smallest separation of a Flibe-coated wall from the target is 3.5 m, so the maximum x-ray fluence and intensity at the liquid Flibe surface are  $46.7 \text{ J/cm}^2$  and  $46.7 \text{ GW/cm}^2$ , respectively. The x-rays vaporize  $2.35 \text{ mg/cm}^2$  or  $11.9 \text{ }\mu\text{m}$  of Flibe from the wall. The base case results are all 18% higher. The x-rays also create a high pressure gradient in the vapor that drives a shock wave into the vapor. This shock can be seen in Fig. 2.7, where Lagrangian zone boundaries that are fixed in the material are plotted against time. The shock propagates through the vapor, which is at or slightly above the liquid density of the liquid, and eventually reaches the vapor/liquid interface in the Flibe. In Fig. 2.8, we have added pressure contours to Fig. 2.7. This figure shows that pressures of several tens of GPa are generated in the material.

**Table 2.4. Parameters on the Closest Wall of the Osiris Target Chamber**

	<b>Assumed</b>	<b>Base Case</b>
Wall Material	Flibe	Flibe
Distance From Target (m)	3.5	3.5
Yield (MJ)	365	432
X-Ray Fluence on Wall (J/cm <sup>2</sup> )	46.7	55.3
X-Ray Intensity on Wall (GW/cm <sup>2</sup> )	46.7	55.3
Vaporized Mass / unit area (mg/cm <sup>2</sup> )	2.35	2.78
Vaporized Thickness (μm)	11.9	14.1
Total Vaporized Mass (kg)	3.6	4.3
Impulse on Wall (Pa-s)	75.6	89.5
Peak Pressure (GPa)	31.2	36.9

The issue of where the vapor flows has yet to be analyzed in detail. The Osiris chamber has been designed to direct the flow of the vapor downward into the condensing spray and pool. The spray provides a very large surface area of Flibe at the cold leg temperature. The condensation of material onto spray droplets can be analyzed, but it was outside the scope of the current study. We must assume that the spray injection system can be adjusted to provide enough droplet surface area to reduce the vapor density to the proper level before the next shot. We must design the system to condense ~ 4 kg per shot, so we must inject a least a few kg of spray per shot to absorb all of the latent heat of vaporization.

Another concern is the flow of vapor into the beam ports. Condensed liquid in the beam tubes could drip into the path of the heavy-ion beams and prevent them from reaching the target. We are relying on the shape of the reactor chamber to direct the flow of vapor away from the beam ports, but some material transport down the beam tubes is unavoidable. An estimate of how much material will flow into the ports will require a three dimensional simulation of the vapor flow and condensation in the target chamber. One can imagine several solutions to this problem. Condensation of the vapor onto particular surfaces could be achieved by controlling the temperatures on the port walls. Surfaces above the beams could be heated to prevent condensation in critical areas.

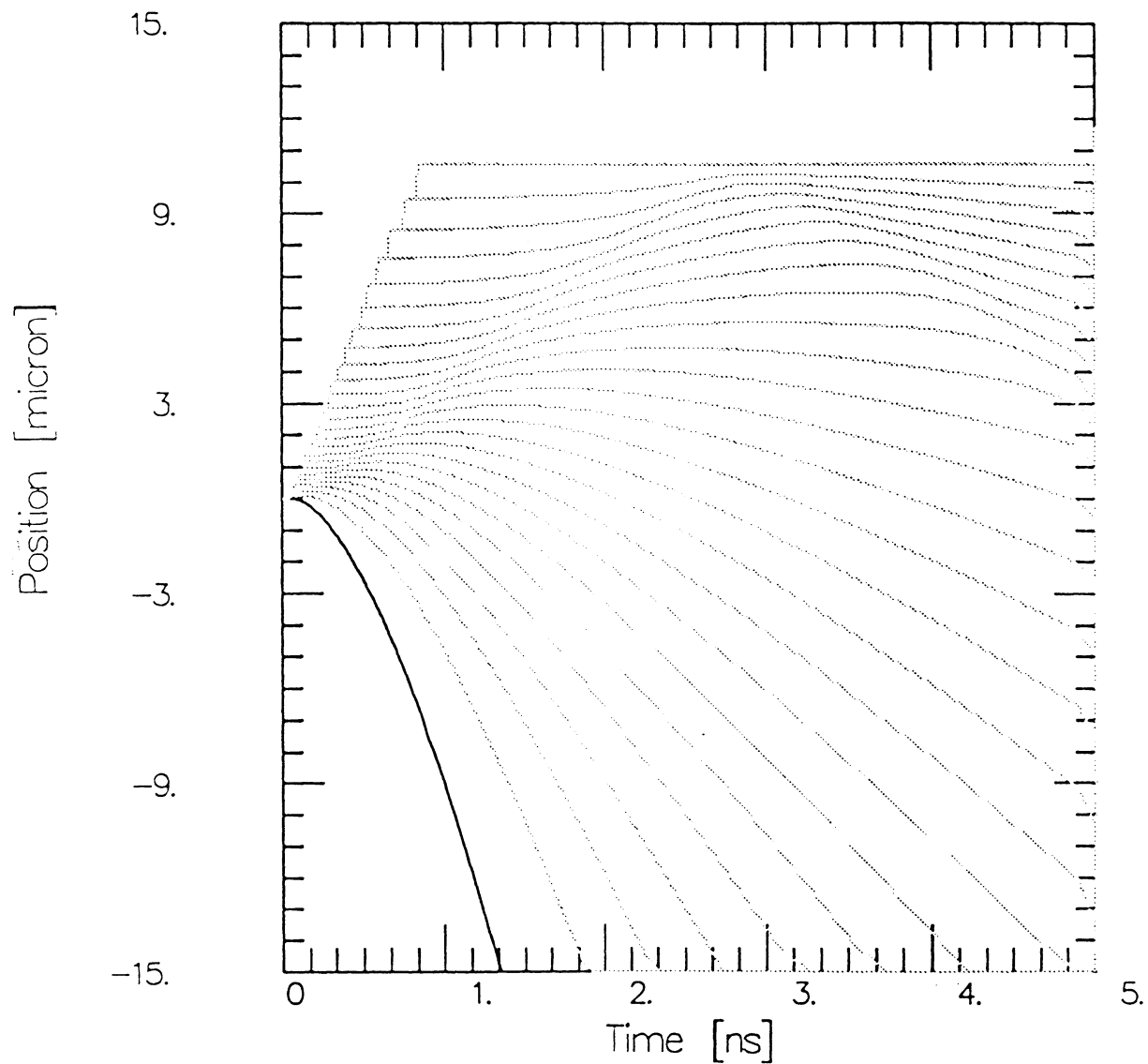
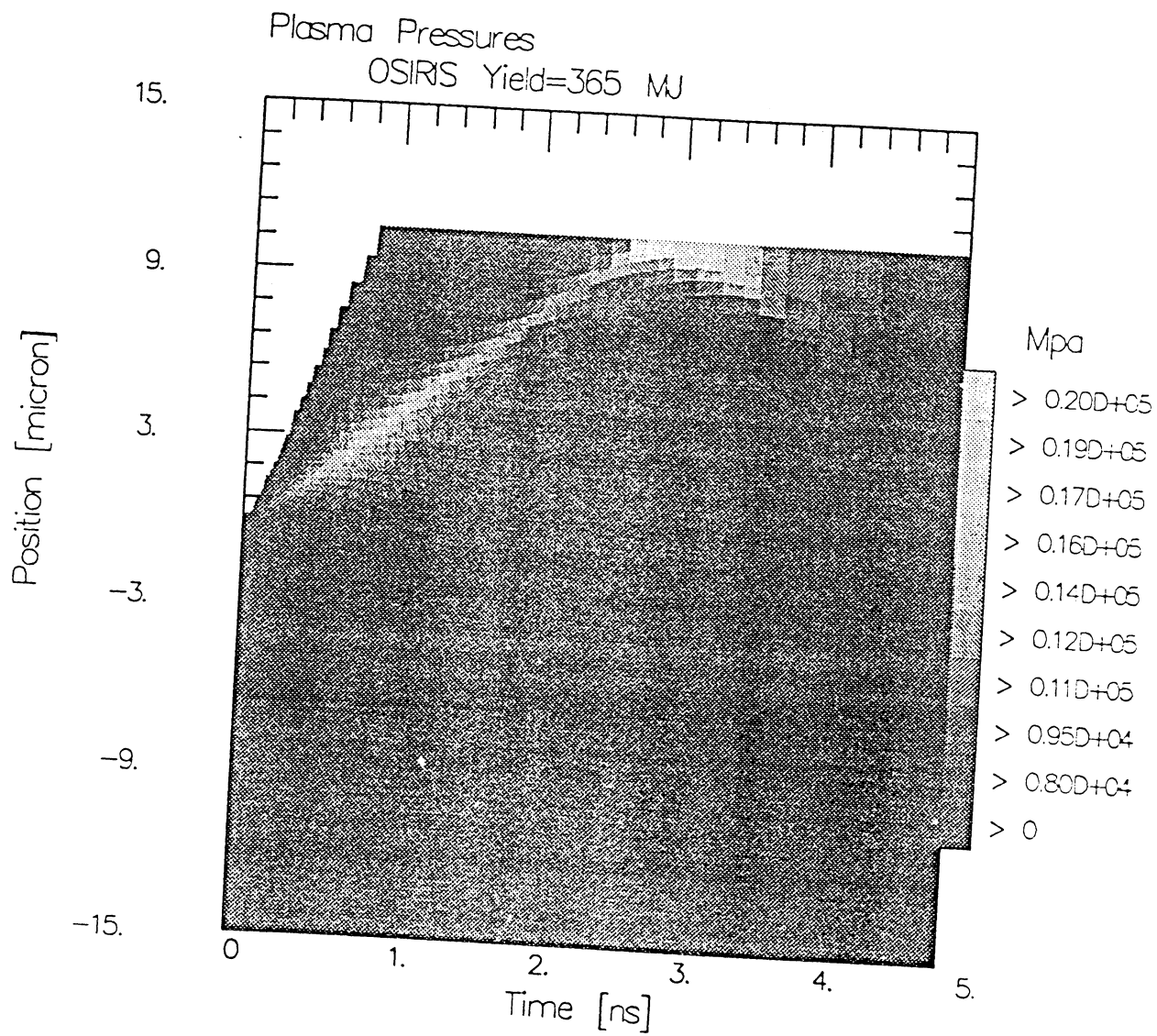


Fig. 2.7. Positions of Lagrangian Zone boundaries vs. time for vaporization from the Osiris first wall. Position equals 0 is the original position of the liquid surface of the Flibe. All other positions are in  $\mu\text{m}$ .



**Fig. 2.8.** Pressure contours for Osiris assumed conditions overlaid on Fig. 2.7. Position equals 0 is the original position of the liquid surface of the Flibe. All other positions are in  $\mu\text{m}$ .

#### 2.2.2.4 Wall Mechanical Loading

The pressure at the interface is shown as a function of time in Fig. 2.9. The peak pressure at the interface is 31.2 GPa, which is enough to launch a shock into the liquid Flibe. The impulse at the interface is 75.6 Pa-s, so the effective pulse width is 2.4 ns. This impulse is smaller than that used in several IFE reactor designs. Since the impulse and peak pressure are proportional to the target yield, the "Base Case" impulse is estimated to be 89.5 Pa-s, and the corresponding peak pressure is 36.9 GPa.

The propagation of shocks deeper into the liquid Flibe has yet to be analyzed. Computational tools are available to analyze this, and the work has been proposed as a follow-on task. Issues to consider are the splashing of liquid Flibe from the surface and propagation to the shock into the substrate material. The splashing of Flibe could leave the substrate material unprotected from the next shot. It could also generate slow-moving droplets to interfere with the next burst of heavy-ion beams. The imparting of shock to the substrate material could damage the material over time and shorten its lifetime.

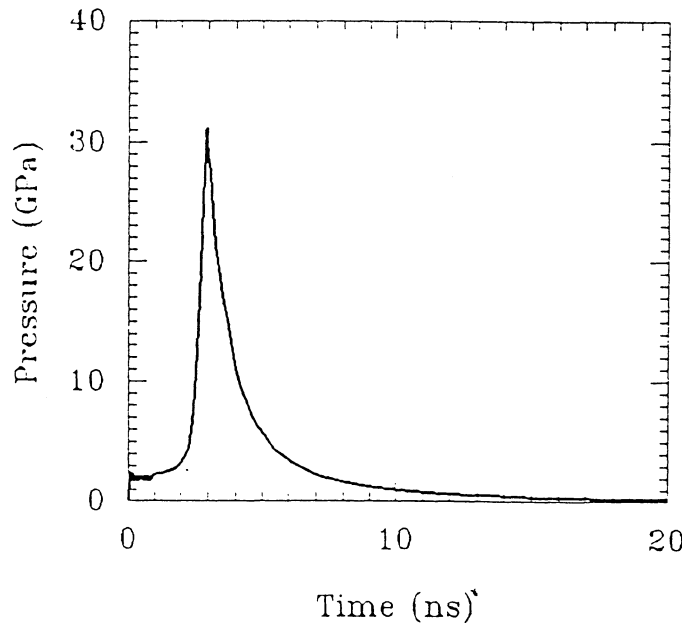


**Fig. 2.9.** Pressure at the vapor/liquid interface on the closest Flibe-coated wall of the Osiris target chamber.

### 2.2.2.5 Flibe Flow Through Fabric

The Flibe weeps through the carbon fabric to the first wall surface, as seen in Fig. 2.1, providing a protective layer. The weep rate controls the buildup of Flibe on the surface. This rate must closely match the vaporization rate from target x-ray and debris energy. Too high a weep rate will produce a thick film of Flibe, which will run down vertical surfaces and drip off horizontal ones. Too low a weep rate could leave the carbon exposed to damage.

It may actually be preferable to have too little Flibe than too much. The Flibe absorbs the softest portion of the X-ray spectrum, leaving the x-rays which pass into the lower-Z carbon harder (having higher average energy) as well as reduced in intensity. Some volumetric heating in the carbon should be acceptable, provided this heat is low enough to be conducted to the coolant without excess thermal stresses. This approach was discovered toward the end of this study, and there has not been time for any analysis; however, it seems worth pursuing.

**Wetting.** Flibe does not wet carbon; therefore, it would bead up on a flat plate of carbon since its surface tension, 0.2 N/m, is quite high even at 600°C. (It is about half the surface tension of mercury at 20°C.) The pore spacing in the carbon fabric can be very fine, so the Flibe may wet itself and form a uniform surface film held in place by the Flibe strands in the pores. This mode of attaching the film is critical because stress waves due to blowoff can otherwise knock the film off the carbon. While it would be quickly replaced, free-falling Flibe would be vaporized, increasing chamber density to excessive levels for beam propagation. Simple experiments using pulsed lasers could address a number of these issues.

If wetting is required to maintain the Flibe film on the carbon, a monolayer film of metal may be needed on the first wall surface. Tungsten, tantalum, and molybdenum have thermal expansion coefficients close to carbon. While this would induce some radioactivity, the volume of activated material would be small because the film is so thin. For example, with a first wall surface area of 150 m<sup>2</sup>, a monolayer film 5Å thick would have a volume of only about 0.08 cc. How this high-Z film responds to x-ray shine-through needs to be investigated.

**Flow Control.** The Flibe weep rate is governed by the Flibe pressure and surface tension, and the fabric thickness and permeability. The flibe pressure ranges from 70 kPa at the top to 140 kPa at the bottom of the blanket. As mentioned, surface tension is quite high. The capillary pressure drop due to surface tension is<sup>2,7</sup>

$$\Delta P = \frac{4\gamma}{d}$$

where  $\gamma$  is the surface tension in N/m and  $d$  is the pore diameter. If  $d$  is below 10  $\mu\text{m}$ ,  $\Delta P$  reaches the 100 kPa range and the surface tension could block the flow.

The other control variable is carbon permeability. For Reynolds numbers less than 10, which is typical, the bulk flow velocity  $u$  (= volume flow/wall area) is given by Darcy's Law<sup>2,8</sup>

$$u = -\frac{k}{\mu} \frac{dP}{dx}$$

where  $k$  is the permeability in  $\text{m}^2$ ,  $\mu$  the viscosity in newton-sec/ $\text{m}^2$ , and  $dP/dx$  the pressure gradient through the cloth in  $\text{N}/\text{m}^3$ . Permeability is often expressed in darcies (1.0 darcy =  $9.875 \cdot 10^{-13} \text{ m}^2$ ). Note that permeability is not the same as porosity. Porosity  $\epsilon$  is related to permeability  $k$  by the relation:<sup>2,9</sup>

$$k = \frac{\epsilon^3 d^2}{150}$$

A small change in porosity has a large effect on permeability. This equation is approximate and used for rough estimates only. More accurate calculations involve other features, such as connectivity and tortuosity.<sup>2,10</sup> The best action is to measure permeability experimentally.

As discussed in the next section, about 14  $\mu\text{m}$  of Flibe are vaporized each shot, giving a recession rate at 4.6 Hz of  $6.5 \cdot 10^{-5} \text{ m}/\text{sec}$  (assuming no film is knocked loose by the shock waves in the Flibe). This must equal the flow velocity  $u$  above. Given a nominal pressure gradient over a 0.01 m thick wall of  $10^7 \text{ N}/\text{m}^3$  and a Flibe viscosity of  $8 \cdot 10^{-3} \text{ N-sec}/\text{m}^2$ , then a cloth permeability of about  $5 \cdot 10^{-14} \text{ m}^2$  (50 millidarcies) is needed. Note that this is actually 50 millidarcies per cm fabric thickness. A thicker fabric can have higher permeability.

Estimates of required fabric porosity and pore size can be made by combining the above equations, which gives a quadratic in  $1/d$ :

$$\frac{150 u \mu t}{\epsilon^3} \left[ \frac{1}{d} \right]^2 + 4 \gamma \left[ \frac{1}{d} \right] - \Delta P = 0$$

Figure 2.10 shows solutions to the last equation for 2 and 10 mm fabric thicknesses. The curves

asymptote to  $d = 8 \mu\text{m}$ , which is the point at which capillary action blocks the flow for a nominal 100 kPa pressure drop across the fabric. Woven cloths generally have porosities of at least 10-20%. Contemporary carbon fabrics tend to be much higher, over 50%, because they are woven with the intention of being infiltrated with a matrix material like epoxy. But there is no reason why carbon can't be woven very tightly, like a seatbelt. Then porosities would be in the 10-30% range, and pore sizes could be in the 15-100  $\mu\text{m}$  range, depending on fabric thickness. For example, with 2 mm thickness and 30% porosity, mean pore size must be around 15  $\mu\text{m}$ . With tightly woven fabric, individual yarns are several times the pore size. In this case, yarn diameter might be in the 100  $\mu\text{m}$  (.004") range, or about the thickness of ordinary sewing thread.

Considering the above, it appears likely that the proper range of Flibe weeping can be achieved with carbon cloth that is tightly woven using techniques commonly used for other cloth materials. Considerable fine tuning would be required to account for differences in pressure drop and vaporization depth at different points on the first wall. But the concept appears feasible, especially when one exploits the combined effects of permeability and surface tension.

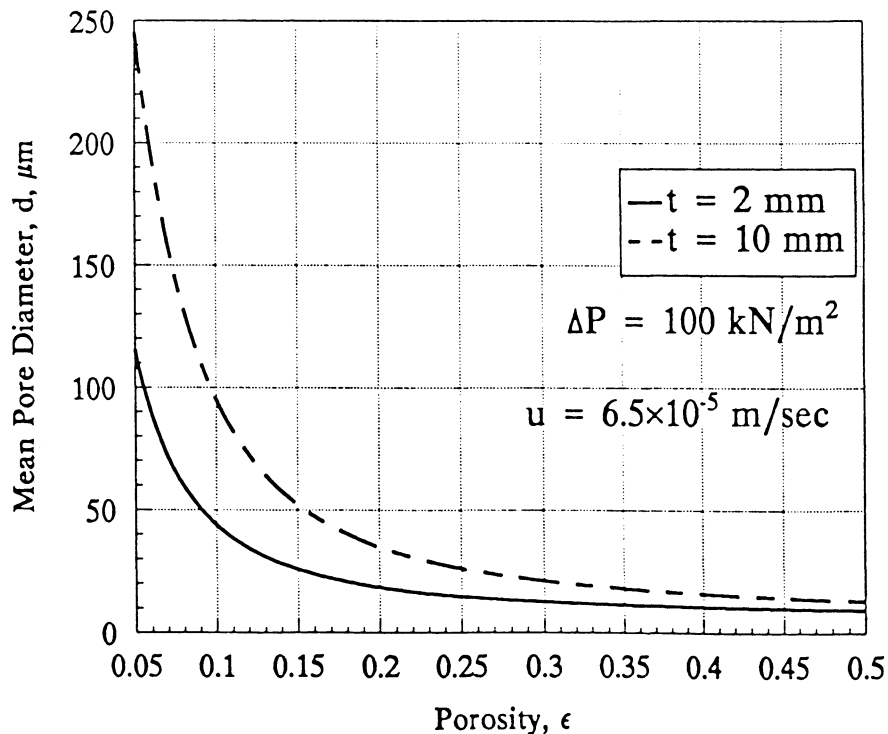


Fig. 2.10. Allowable cloth porosity vs. pore size for two cloth thicknesses. With the nominal head of the Flibe in the blanket, flow is just sufficient to maintain a protective surface of liquid Flibe.

### 2.2.2.6 Condensation of Vaporized Flibe

There are two issues relating to vapor condensation: (1) pumping of the vapor so that it contacts the cold liquid spray and pool and (2) the ability of this liquid to condense the vapor without overheating. In this section we examine these issues.

**Vapor Pumping.** The pumping speed,  $s$ , of the vapor through an area  $A$  just above the spray is given by<sup>2,11</sup>

$$S = \frac{62.5 A_{cm^2}}{\sqrt{M}} \sqrt{\frac{T_K}{298}} \quad //s$$

where  $M \approx 14$  is the average molecular weight of dissociated Flibe, and  $T$  is the vapor temperature, about 2 eV (23,000 K). The pumpdown time,  $\tau$ , is given by

$$\tau = 2.3 \frac{V}{S} \log \left[ \frac{n_1}{n_2} \right]^{1.67} \quad \text{sec}$$

where  $V$  is the vapor volume in liters, and  $n_1$  and  $n_2$  are the initial and final vapor densities, respectively, in  $m^{-3}$ .

With 129 MJ fusion surface energy per shot (as discussed in Section 2.2.2.3), about 4.3 kg of Flibe is vaporized. With a nominal 300  $m^3$  vapor volume,  $n_1$  (of undissociated Flibe) is  $6 \cdot 10^{23} m^{-3}$ . This must be brought down to  $4.8 \cdot 10^{18} m^{-3}$  in the 220 msec available between shots. Using the two equations above gives  $\tau = 60$  msec, allowing plenty of margin.

**Vapor Condensing.** The Flibe vapor is condensed by direct contact with the spray and the pool. A number of processes are occurring here simultaneously: (1) High turbulence levels provide mixing, which reduces the liquid surface temperature; (2) The spray, pool, and the interaction between them increase the surface area available for condensation. (3) The expansion of the vapor cools it to the point of condensation into high speed droplets, which impact the pool and distribute their considerable kinetic energy to some depth. We estimate the ability of each of these processes to condense the vapor acting alone, knowing full well that there are complementary synergistic effects.

As seen above, the vapor may impact the liquid pool so quickly that condensation does not occur. If this happens, some liquid will be vaporized and condensed at a later time, thus spreading out the heating of the liquid with time.

The degree of turbulence needed in the pool depends on the heat flux and the allowable temperature rise. The target nonneutron energy is 129 MJ, all of which is assumed to go into Flibe vapor. The interpulse time is 0.22 sec. The pool disc area (ignoring the sprays for the moment) is about 95 m<sup>2</sup>. Therefore, the needed condensing power is  $q_s = 6.3 \text{ MW/m}^2$ . If the pool were quiescent, heat would be removed by thermal conduction alone, and the surface temperature rise,  $\Delta T_s$ , in time,  $\tau$ , would be<sup>2,12</sup>

$$\Delta T_s = 2 q_s \sqrt{\frac{\tau}{\pi \rho K C_p}}$$

where  $\rho$ ,  $K$ , and  $C_p$  are the Flibe density (2000 kg/m<sup>3</sup>), thermal conductivity (1.0 W/m-K), and heat capacity (2380 J/kg-K), respectively. For  $\tau = 0.22 \text{ sec}$ ,  $\Delta T = 1520 \text{ K}$ , an unacceptably high temperature rise. Turbulent mixing is clearly required.

A measure of turbulence is the Nusselt number  $Nu = hD/K$ , where  $h$  is the convection heat transfer coefficient and  $D$  is a characteristic dimension. This number is essentially a ratio of the apparent thermal conductivity during turbulent flow to thermal conductivity with a static liquid. Since Flibe has such a poor thermal conductivity, but has a fairly low viscosity, turbulence can greatly improve heat flow.

As seen in the above equation, surface  $\Delta T \sim \sqrt{1/K}$ . The Nusselt number needed to reduce the liquid surface temperature rise from 1520 K to an acceptable 50 K is then

$$Nu = \left[ \frac{\Delta T_1}{\Delta T_2} \right]^2 = \left[ \frac{1520}{50} \right]^2 = 900$$

This value is not difficult to achieve with Flibe. The Nusselt number is related to fluid flow by<sup>2,13</sup>

$$Nu = 0.036 Pr^{0.33} Re^{0.8}$$

where  $Pr = \mu C_p / K$  is the Prandtl number (19 for Flibe), and  $Re = \rho u D / \mu$  is the flow Reynolds number with  $D$  as the channel characteristic dimension. Because of the complexity of the flow, the choice of  $D$  is not clear; but it is taken here to be 50 cm, beyond which one would expect the flow to be fully developed. The required Reynolds number for  $Nu = 900$  is  $Re = 95000$ .

the choice of  $D$  is not clear; but it is taken here to be 50 cm, beyond which one would expect the flow to be fully developed. The required Reynolds number for  $Nu = 900$  is  $Re = 95000$ . The required characteristic velocity is only 0.8 m/sec, which would be readily exceeded. Therefore, pool turbulence alone is sufficient to condense the vapor.

The second process aiding condensation is the multiplication of the pool area by the sprays and the impact of the sprays on the pool. The relationship between temperature rise and heat flux given earlier can be used to calculate the required surface area. To reduce the surface  $\Delta T$  from 1520 to 50 K, would require a heat flux reduction of about 30 to 1. This is the increase in surface area from the sprays and splashing required relative to a flat pool surface. This intuitively appears a little high, and it is unlikely that area multiplication alone can condense the vapor. It should, however, assist the other mechanisms.

The third condensation mechanism deals with the observed fact<sup>2,14</sup> that expanding blowoff vapor cools adiabatically and condenses to form high-speed droplets. These can impact the pool and distribute their energy to a considerable depth. The depth  $\delta$  required to limit temperature rise to 50 K is

$$\delta = \frac{E_{surf}}{\rho A_{pool} C_p \Delta T}$$

which, for 129 MJ target surface energy, is about 6 mm. This depth is small enough that it appears to be achievable.

The combination of mechanisms discussed above appear likely to provide condensation of the vaporized Flibe within the interpulse time. In fact, droplet impact alone may be enough, which would eliminate the need for high pressure sprays. Simple experiments would provide much of the necessary data to determine which of the mechanisms discussed above are required.

## 2.2.3 First Wall Design

### 2.2.3.1 Fabrication and Assembly

The first wall is integral with the blanket support and consists of tightly-woven carbon cloth. Three cloth layers are used to make up the two Flibe flow channels, and front and back are stitched together with cloth radial cross members. This is shown in Fig. 2.11. Note that it resembles an air mattress in cross section. It looks externally like a peeled orange. This arrangement minimizes tensile stresses in the cloth from the Flibe pressure.

The critical radius for tensile stress is the radius of curvature for the individual blanket cells, and this varies with azimuthal angle reaching a maximum at the equator. If the radius of curvature is 2 m there, then a 5 mm thick cloth is stressed in tension to about 100 MPa with a Flibe pressure of 250 kPa. The flow contribution is negligible compared to the static pressure. This assumes an inlet duct pressure of 70 kPa. This is only about 5% of the strength of the P-100 fiber that is discussed below.

### 2.2.3.2 Expected Neutron Lifetime

An example carbon fiber that would work here is P-100, made by Union Carbide. It has shown very good resistance to fast neutrons to a fluence of  $5 \cdot 10^{21}$  n/cm<sup>2</sup>. As shown in Table 2.5, irradiation leads to little dimensional or modulus change, and actually increases strength. This is just one of many types of carbon fibers that may be suitable. Another is vapor-grown carbon fiber, developed by Endo in Japan and General Motors.<sup>2,15</sup> Versions of this fiber have also been tested under neutron irradiation<sup>2,16</sup> and perform even better than P-100.

**Table 2.5. Neutron Irradiation Data for P-100 Carbon Fibers**

Maker	Union Carbide
Type fiber	P-100
Annealing temperature	3100°C
Exposure temperature	620°C
Total neutron dose	$5 \cdot 10^{21}$ n/cm <sup>2</sup>
Neutron energy	> 50 keV
Length change	-1.1%
Diameter change	+1.5%
Modulus before irradiation	586 GPa
Modulus after irradiation	565 GPa
Tensile strength before irradiation	2.0 GPa
Tensile strength after irradiation	2.4 GPa

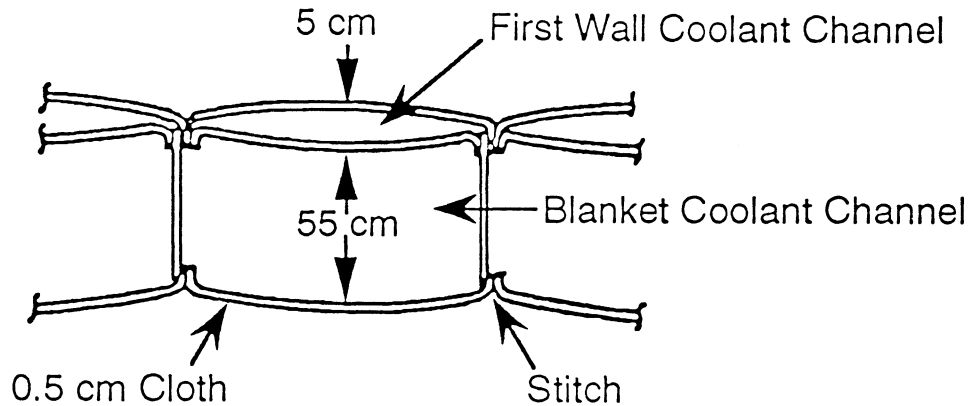


Fig. 2.11. Air mattress cross section of the blanket used to minimize hoop stresses.

### 2.2.3.3 Changeout Procedure

As discussed above, it is expected that the Osiris blanket will have to be changed out about once a year. An advantage of this concept is that the entire lightweight assembly, drained of Flibe, can be removed from the top. Routine in-chamber access is not required. The steps in this process are listed below.

1. After reactor shutdown, the Flibe is automatically drained through small holes in the blanket into the pool. Some recirculation of the Flibe may initially be required until the short-term afterheat has dissipated from the blanket fabric. Heaters in the bottom of the pool keep that Flibe molten, but any Flibe remaining in the blanket fabric is allowed to solidify. Since Flibe does not wet carbon, little will remain anyway. (5 days effort)

2. The low and high pressure Flibe inlet pipes at the top of the reactor are disconnected. To avoid interference, the break point in the upper pipe must be further from the reactor centerline than the lower, and both must clear the vacuum chamber cover. (2 days)

3. The vacuum chamber cover is unbolted from the vacuum chamber. (3 days)

4. The vacuum chamber cover is lifted out and the attached drained blanket fabric, supports, and high pressure manifold are transported to the hot cell. Note that all the interior

hardware clears the driver focussing magnets. After cooldown, the fabric structure along the first wall can be removed and prepared for shallow burial storage. The remaining hardware that was shielded from the primary neutrons, including the high pressure manifold, can probably be reused after refurbishing. (3 days)

5. The new blanket assembly and vacuum chamber cover are installed simply by lowering it into place, reversing the steps above. To avoid cold-trapping, the Flibe in the pool is heated to at least 100° above melting before circulating. (5 days)

The total elapsed time is estimated at 18 days, giving an availability loss of 5%. During that time, other non-interfering maintenance can also be performed. In addition to the reactor hall, a hot cell room, a spare blanket storage room, and a new blanket assembly room are needed. The first three rooms will each be 16 by 16 meters, and the new blanket assembly room will be 16 by 32 meters. The increased size of the assembly room allows for large component laydown space prior to assembly. Some of these activities can take place in the same area at different times.

## **2.2.4 Blanket Design**

### **2.2.4.1 Use of Flibe**

Two great advantages of flowing lithium-bearing coolants are the simplicity of the blanket and the fact that only an empty shell needs to be periodically changed out. For the pulsed loadings inherent in IFE, a further advantage is the ability of the coolant to carry damaging shocks away from the first wall and dissipate them. This occurs because shocks from x-ray blowoff are very short in duration. As they propagate, they automatically spread out and diminish in amplitude. Because Flibe and graphite have comparable acoustic impedances, reflections at interfaces are minimal.

There are three coolant choices: pure lithium, lithium-lead ( $\text{Li}_{17}\text{Pb}_{83}$ ) or Flibe ( $\text{Li}_2\text{BeF}_4$ ). The first two could certainly be considered, but lithium is very reactive and is very combustible in air, and lithium-lead has high density and a problem with activation of the lead. Flibe, on the other hand, is quite inert; the activation of fluorine is much less than that of lead. Flibe also makes a good coating material for the first wall because its combination of low atomic number and low vapor pressure allows its use at high temperatures and low chamber pressures needed for heavy-ion beam transport.

Table 2.6 shows pertinent properties of Flibe. It has a high melting point, 460°C, but a low thermal conductivity, 1.0 W/m-K. While it will be necessary to keep pools of it molten during down periods, the heat that must be supplied should not be great. In the event of loss of flow, the system should be designed to automatically drain Flibe out of the ducting into the pool or a separate hotwell. This can be done for ducts above the reactor by having small permanent drain holes in the bottom of the blanket. During operation, the Flibe flowing through these holes would be negligible compared to the volume of Flibe flowing through the blanket. To drain all of the ducting and the IHX to the pool would require the reactor to be the lowest point, which would be rather inconvenient. Alternately, ducts can be jacketed to accept hot gas or liquid heating. In any case, with good insulation and the poor Flibe conductivity, the amount of heating needed should be small.

**Table 2.6. Properties of Liquid Flibe<sup>2,17</sup>**

Percent LiF	67
Percent BeF <sub>2</sub>	33
Melting Temperature	459°C
Density	2000 kg/m <sup>3</sup>
Specific Heat	2380 J/kg-K
Thermal Conductivity	1.0 W/m-K
Viscosity at 600°C	8·10 <sup>-3</sup> Pa-s
Prandtl Number at 600°C	19
Heat of Fusion	448 kJ/kg
Heat of Vaporization	5.54 MJ/kg
Surface Tension at 600°C	0.2 N/m
Approx Cost for Large Quantities	\$84/kg

The viscosity of Flibe is about that of liquid water at room temperature. The high Prandtl number is due to the low thermal conductivity. Convective heat transfer coefficients can be quite high, and Flibe is actually a fairly good convector of heat although it is a poor conductor.

The surface tension is quite high, about half that of mercury at room temperature. This feature was exploited to limit the weep rate through the first wall fabric. Because Flibe does not wet carbon, a thin metal coating may be needed to get a uniform film on the surface, as discussed earlier in this chapter.

#### 2.2.4.2 Flibe Flow Issues

**Low Pressure Flibe.** After the initial vaporization of surface Flibe, further vaporization occurs until an equilibrium pressure is reached where the saturation temperature at the liquid Flibe surface corresponds to the Flibe vapor pressure in the chamber. As discussed above, the acceptable density for beam propagation corresponds to a Flibe saturation temperature of 570°C. The bulk Flibe temperature below the surface must be below this or equilibrium will be reached at a higher temperature. This is the reason for the two flow channels in the blanket. The Flibe in the first, very thin channel, is moving very quickly, picks up little neutron heating, and increases to only 520°C. Most of the neutron heat is picked up by the Flibe in the second, much slower, pass up the back of the blanket.

The Flibe in the high-speed channel has a nominal Reynolds number of 66,000, making it quite turbulent. Heat transfer to the first wall channel is low, because most of the nonneutron energy goes to the pool. The hydrostatic head from top to bottom of the blanket is 137 kPa, compared to 49 kPa flow pressure drop in the first channel. The second figure is then the required inlet pressure to the blanket. After the second turn, the flow pressure drop is nil, and with the 49 KPa inlet pressure, the Flibe exits into vacuum at zero pressure. There would be no difficulty in increasing the Flibe pressure in the blanket to have some residual pressure so that the Flibe exiting the blanket can be sprayed into the vacuum, enhancing tritium release.

**High Pressure Flibe.** Flibe enters the reactor chamber in two flow streams: the low pressure blanket stream discussed above and the high pressure stream that sprays into the pool. The high pressure is due to the short in-flight time needed to keep the spray from overheating. This time is taken to be 0.13 sec, about half the dwell time between shots. Since it must traverse about 6 m, the spray velocity is 46 m/sec. The nozzle pressure is  $\rho v^2/2 = 2.1$  MPa.

The spray supplies all of the pool flow; the side blanket is dumped directly to the exit manifold. The pool absorbs all of the nonneutron energy plus about 12% of the neutron energy, for a total power of ~950 MW. The desired exit temperature is 650°C. But another 5.5% of the neutron power is absorbed in the annular exit manifold. The design exit temperature from the pool should then be about 640°C. For this 140° temperature rise, the mass flow in the spray must be ~2300 kg/sec. The ideal pumping power for the spray is 3.0 MW. Note that this power is also counted as heat addition.

### **2.2.4.3 Blanket Changeouts**

The key blanket issues during changeout are draining of the Flibe in the blanket and upper ducting, and preventing solidification of Flibe remaining in the pump and IHX. Fortunately, Flibe is such a poor conductor that solidification takes a long time. For example, it can be shown<sup>2,9</sup> that, in an uninsulated 1.0 m diameter duct carrying Flibe at 500°C, at least one week would be needed to cool the Flibe half way through to the solidification temperature. Adding insulation and accounting for the latent heat of fusion should increase this time several fold. At the worst, insulated ducts wrapped in heater tape will keep the Flibe liquid. With 20-cm-thick pipe insulation, heater tape must supply a modest 200 W/m<sup>2</sup>.

The Flibe in the pool can be maintained liquid by heating elements at the bottom. Even if the top surface solidifies, solid particles will sink and provide circulation for the heater. Because hot Flibe vapor can get into the building atmosphere while the cover is off, some sort of filtration system will be needed.

## **2.2.5 Vacuum Vessel Design**

### **2.2.5.1 Description of Vacuum Vessel**

The vacuum vessel is 13 m diameter by 11 m high. It consists of a 5 cm thick cylinder 8.5 m high, a 13 m diameter base 7 cm thick, and a 13 m diameter conical cover 2 m high that is also 7 cm thick. Loads from the one atmosphere overpressure are compressive and quite low, about 14 MPa. It is shielded from both primary and secondary neutrons by the main and cascade flow blankets. It should, therefore, last the life of the plant.

### **2.2.5.2 Vacuum Vessel Materials**

There is a wide variety of acceptable materials for the vacuum vessel, although there will be enough neutron fluence that low activation materials are preferred. Because it is in contact with the Flibe, the chamber will run quite hot. One material that will work is carbon or silicon carbide composite with the inevitable porosity sealed by infusing it with Flibe. As long as the outside of the vessel remains below 460°C, the Flibe will stay solid and provide a vacuum seal. The total chamber mass is about 80,000 kg. Assuming a unit cost of the composite to be \$100/kg, the total vacuum vessel cost is about \$8 million.

There are certainly other material choices, such as austenitic or ferritic stainless steels, which are less expensive and easier to fabricate. While they will last the life of the plant, they will introduce a substantial gamma ray source that will require additional shielding. There are a number of possible vessel design options, so the choice of vessel material is not an important feasibility issue for the Osiris design.

## **2.2.6 Neutronics Analysis**

### **2.2.6.1 Neutronics Model and Assumptions**

Neutronics analysis was performed using a spherical geometry model to simulate the Osiris fusion power reactor. The compressed DT target was included in the neutronics calculations with the DT source neutrons uniformly distributed in a 0.1 mm radius region of DT at 300 g/cm<sup>3</sup> density. Target materials surrounding the DT core are not included in the model due to their small impact on neutronic parameters. Neutronics calculations were performed with the one-dimensional discrete ordinates transport code ANISN.<sup>2.18</sup> A coupled 30 neutron - 12 gamma group nuclear data library, MATXS5, based on ENDF/B-V cross section files was employed.<sup>2.19</sup> All calculations were performed with P<sub>3</sub>S<sub>8</sub> approximations.

Table 2.7 shows the regional dimensions and materials in a spherical geometry model used for scoping and optimization analyses.

### **2.2.6.2 Blanket Design Optimization**

Neutronics calculations were performed parametrically (varying the blanket thickness  $x$ ) for the scoping model shown in Table 2.7. The results are presented in Figs. 2.12 - 2.15 and discussed below.

Figure 2.12 depicts the tritium breeding ratio (TBR) and overall energy multiplication of the scoping Osiris system as a function of total Flibe zone thickness. Note that the overall energy multiplication,  $M_o$ , here is defined as the total energy deposited per DT reaction divided by 17.6 MeV. The total energy includes neutron energy deposited in the target, blanket, and other structures, and the alpha particle energy. In these calculations, natural lithium (7.42% in <sup>6</sup>Li) is employed. (Enriching in <sup>6</sup>Li to 20% would probably give better results when the Flibe zone thickness is less than 0.5 m.)

Two observations can be made for TBR and  $M_0$ : (1) In addition to the graphite vessel, which is 0.2 m thick, a graphite reflector/shield would be helpful in enhancing both TBR and  $M_0$ , particularly when the total Flibe zone thickness is less than 0.5 m, and (2) the TBR and  $M_0$  are near their asymptotic values when the total Flibe zone thickness is  $>0.5$  m.

**Table 2.7. Osiris Neutronics Problem Description**  
**Geometry: 1-D spherical**

Region	Description	Material	Inner radius (cm)	Outer radius (cm)	Thickness (cm)
1	Target	DT	0.0	0.01	0.01
2	Inner vacuum	Flibe Vapor	0.01	350.0	350.0
3	Surface Film	Liquid Flibe	350.0	350.2	0.2
4	Panel inner wall	Carbon Fabric	350.2	350.5	0.3
5	Panel coolant	Liquid Flibe	350.5	365.5	15.0
6	Panel outer wall	C-fabric	365.5	365.8	0.3
7	Spray zone	Flibe vapor	365.8	450.0	84.2
8	Neutron blanket wall	C-fabric	450.0	450.3	0.3
9	Neutron blanket	Liquid Flibe	450.3	450.3 + x	x
10	Vessel wall	Carbon	450.3 + x	470.3 + x	20.0

**Materials Compositions**

Material	Density (g/cm <sup>3</sup> )	Element	Atom Fraction
Target	300.0	D	0.5
		T	0.5
Flibe (2LiF + BeF <sub>2</sub> )	2.0	<sup>6</sup> Li	0.0211
		<sup>7</sup> Li	0.2646
		F	0.5714
		Be	0.1429
Carbon fabric	1.7	C	1.00
Carbon vessel	1.7	C	1.00

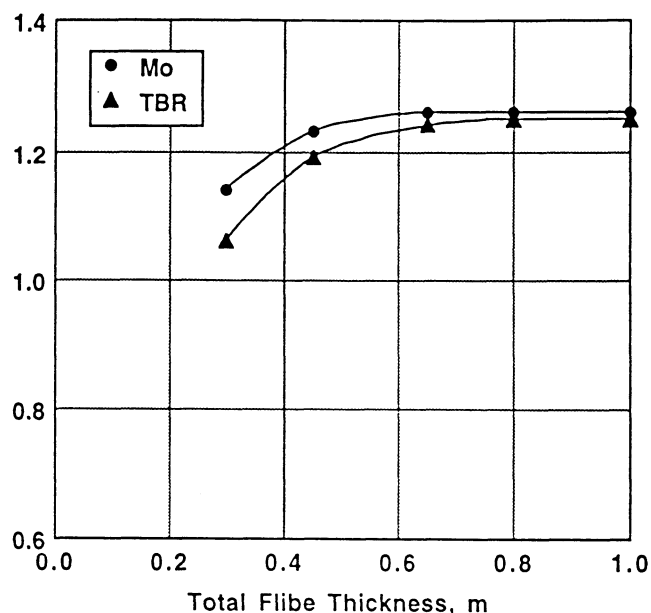


**Fig. 2.12. Tritium breeding ratio and overall energy multiplication factor as a function of Flibe thickness.**

Figure 2.13 gives the nuclear energy deposited in the graphite vessel and total energy leakage as a function of total Flibe zone thickness. The total energy leakage converges to the energy deposited in the vessel when the total Flibe zone thickness is thick enough.

Observations obtained from the analysis shown in Fig. 2.13 are (1) the energy leakage decreases as the total Flibe zone thickness increases, and (2) the nuclear energy deposited in the vessel is 20 MW when the total Flibe zone thickness is 0.5 m (0.35 m neutron blanket, Region 9). Note that here we assume the total fusion power in the scoping Osiris is 2200 MW; after further analysis, the reference fusion power level was reduced to ~2000 MW. The energy deposited in the vessel represents only 0.75% of the total thermal energy when the total Flibe zone thickness is 0.5 m.

Figure 2.14 displays the spatial power density distribution in the scoping Osiris reactor components. The total fusion power assumed is 2200 MW, and the total Flibe zone thickness is 0.45 m. The maximum power densities in the carbon fabric, Flibe, and the graphite vessel are ~ 34, 70, and 1 w/cm<sup>3</sup>, respectively. Maximum neutron wall loading at the first wall is 9 MW/m<sup>2</sup>.

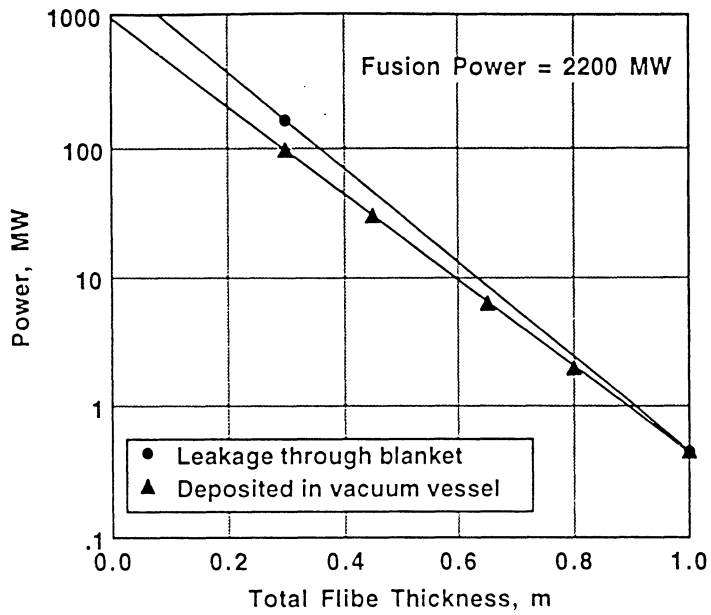


Fig. 2.13. Nuclear power leakage and the vacuum vessel heating as a function of Flibe thickness.

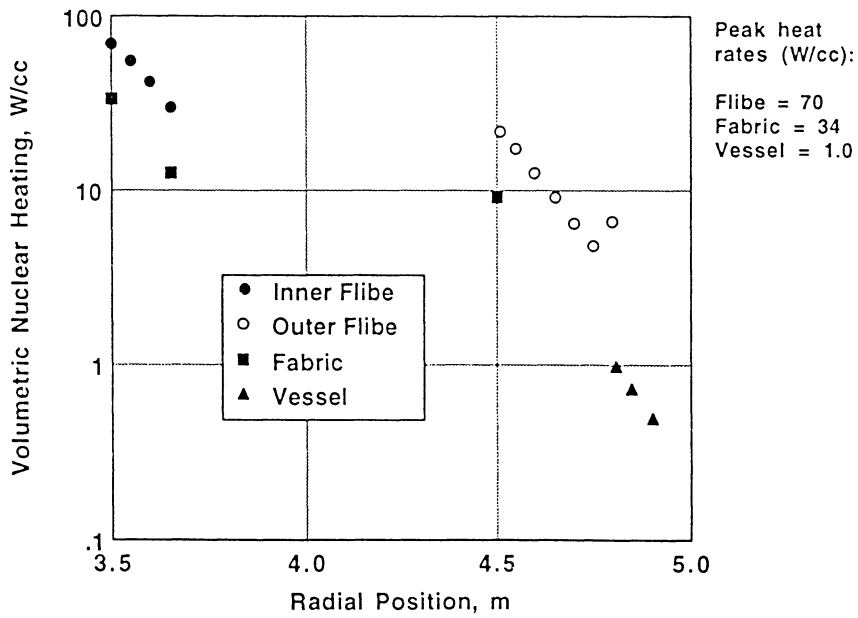


Fig. 2.14. Power density distribution for a 0.45m-thick Flibe blanket.

Figure 2.15 shows the radiation damage parameters in the vessel (maximum numbers) as a function of total Flibe zone thickness. We may conclude that, based on the scoping and optimization design analysis, a design with 0.5 m total Flibe zone thickness is adequate for Osiris.

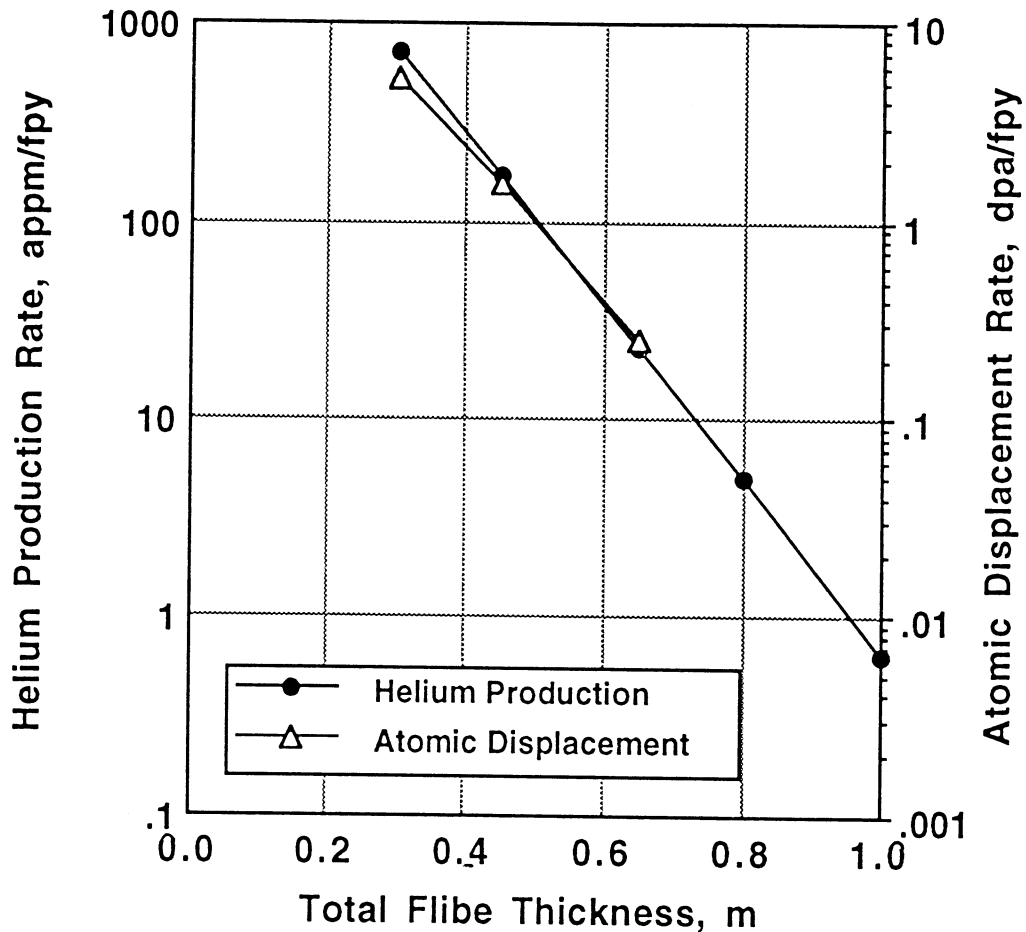


Fig. 2.15. Radiation damage parameters in the vessel as a function of total Flibe zone thickness.

### 2.2.6.3 Neutronics Parameters for Reference Design

Based on the scoping and optimization design analysis performed in Section 2.2.6.2, and other design requirements, the reference Osiris design was determined. Table 2.8 shows the regional dimensions and materials for the reference design. Note that the total Flibe zone thickness in the reference design is 70 cm, more than enough to optimize the nuclear performance of the blanket and provide attenuation protection of the vacuum vessel. Table 2.9 summarizes the tritium breeding and nuclear heating rates in the reference Osiris design.

As shown in Table 2.9, the total tritium breeding ratio is 1.24 tritons/DT neutron, which is more than adequate. The tritium production rate from  ${}^6\text{Li}(n,\alpha)\text{T}$  reaction (T6) is 1.099, while it is 0.137 from  ${}^7\text{Li}(n,n'\alpha)\text{T}$  reaction (T7). The total nuclear heating rate in the Flibe coolant and carbon-carbon composite structure (including the vacuum vessel) is 17 MeV/DT neutron. The nuclear energy deposited in the DT target is 1.75 MeV/DT neutron which will be carried by the target debris to the Flibe first wall film. The sum of the neutron energy deposited in the target is 18.75 MeV/DT neutron. (This results in a target/blanket energy multiplication of 1.33.) If alpha particles are accounted for, the total thermal energy to be removed by the Flibe coolant will be 22.25 MeV per DT neutron (or per fusion reaction). The total energy multiplication  $M_o$ , is 1.26, as shown in Table 2.9. Figure 2.15 displays spatially the volumetric nuclear heating rates in the various reactor components.

Table 2.10 gives the maximum helium production and atomic displacement rates in the carbon-carbon composite fabric and vacuum vessel components. for the Osiris reference design. As shown, the maximum atomic displacement rates in the carbon-fabric first wall and vacuum vessel are 42 and 0.14 dpa per full power year, respectively, while the corresponding helium production rates are 10,600 and 6.1 ppm per full power year, respectively.

#### **2.2.6.4 Biological Shielding**

The biological shielding is an important component to protect the working personnel outside of the reactor chamber, where the biological dose rate during reactor operation should not exceed 2.5 mR per hour. In the Osiris reference design, a steel-reinforced concrete shield (20% mild steel, 70% concrete, and 10% void for gas coolant) of 3 m thick is considered as the biological shield. It is located at 10 m from the target location. Using the concrete and steel compositions given in Table 2.11 we have estimated the operating dose rates outside the concrete shield, as well as behind the carbon vacuum vessel (reactor chamber).

The operating biological dose rate behind the concrete wall is estimated to be about 1.7 mR/h at a fusion power level of 2000 MW. Most of which, about 94%, is due to neutrons. This level of dose rate is lower than the limit, 2.5 mR/h. The biological dose rate behind the chamber, however, is about 55 MR/h which is more than 10 orders of magnitude higher than acceptable.

### 2.2.6.5 Lifetime of Chamber

The radiation damage parameters are shown in Table 2.10, Sec. 2.2.6.3. The atomic displacement and helium production rates in the carbon vacuum vessel are 0.14 dpa and 6.1 ppm per full power year, respectively. The vacuum vessel will last the entire lifetime of the Osiris reactor, since the accumulated displacements per atom there (5.6 for 40 full power years) is more than a factor of 10 lower than the estimated limit, 75 dpa. However, the layers of carbon fabrics inside the vacuum vessel will have to be frequently replaced (every 1.8 full power year) because the maximum atomic displacement rate is 42 per full power year.

**Table 2.8. Neutronics Model for the Reference Osiris Design  
Geometry: 1-D spherical**

Region	Description	Material*	Inner radius (cm)	Outer radius (cm)	Thickness (cm)
1	Target	DT	0	0.01	0.01
2	Inner vacuum	Flibe vapor	0.01	350.0	350.0
3	Surface film	Liquid Flibe	350.0	350.2	0.2
4	First inner wall	Carbon fabric	350.2	350.7	0.5
5	First wall coolant	Liquid Flibe	350.7	355.7	5.0
6	Neutron blanket wall	Carbon-fabric	355.7	356.2	0.5
7	Neutron blanket	Liquid Flibe	356.2	411.2	55.0
8	Neutron blanket wall	Carbon-fabric	411.2	411.7	0.5
9	Cascade repair	Liquid Flibe	411.7	421.7	10.0
10	Spray zone	Flibe vapor	421.7	680.0	258.3
11	Vacuum vessel	Carbon	680.0	700.0	20.0

\*Material compositions are the same as in Table 2.7.

**Table 2.9. Tritium Breeding and Nuclear Heating Rates in the Reference Design  
(Natural Lithium in Flibe)**

<b>Tritium Production Rate (T/DT Neutron)</b>	<b>T6</b>	<b>T7</b>	<b>TT</b>
Region 3 (Surface Film)	0.008	0.002	0.010
Region 5 (1st Wall Coolant)	0.197	0.042	0.239
Region 7 (Neutron Blanket)	0.873	0.093	0.966
Region 9 (Cascade Repair)	0.021	< 0.001	0.021
Tritium Breeding Rates	1.099	0.137	1.236

<b>Nuclear Heating Rate</b>	<b>(MeV/DT Neutron)</b>
Region 1 (DT Target)	1.753
Region 3 (Flibe)	0.181
Region 4 (C-Fabric)	0.210
Region 5 (Flibe)	4.215
Region 6 (C-Fabric)	0.168
Region 7 (Flibe)	12.03
Region 8 (C-Fabric)	0.0032
Region 9 (Flibe)	0.156
Region 11 (Carbon Vessel)	0.0349
Total Energy due to DT Neutrons	18.75
$M_b$ (Blanket + Target Energy)/14.1	1.33
Total Thermal Energy (with $\alpha$ particles)	22.25
$M_o$ (Total System Energy)/17.6	1.26

**Table 2.10. Radiation Damage Parameters in Carbon Fabric and Vacuum Vessel  
(2000 MW Fusion Power; Osiris Reference Design)**

Region	Helium Production Rate (ppm/FPY)	Atomic Displacement Rate (dpa/FPY)
4 Carbon Fabric	10,600	42
11 Carbon Vacuum Vessel	6.1	0.14

[FPY = Full Power Year]

**Table 2.11. Compositions of Steel and Concrete Shield Materials  
(atom densities, x 10<sup>24</sup> atoms/cm<sup>3</sup>)**

Mild Steel (100%)			
C	7.85 x 10 <sup>-4</sup>	N	2.36 x 10 <sup>-5</sup>
Al	5.89 x 10 <sup>-5</sup>	Si	5.21 x 10 <sup>-4</sup>
Mn	4.46 x 10 <sup>-4</sup>	Fe	8.35 x 10 <sup>-2</sup>
Cu	1.19 x 10 <sup>-4</sup>		
Concrete (100%)			
H	1.04 x 10 <sup>-2</sup>	<sup>10</sup> B	3.59 x 10 <sup>-4</sup>
<sup>11</sup> B	1.44 x 10 <sup>-3</sup>	O	3.94 x 10 <sup>-2</sup>
F	2.26 x 10 <sup>-4</sup>	Na	9.83 x 10 <sup>-4</sup>
Mg	1.77 x 10 <sup>-4</sup>	Al	4.43 x 10 <sup>-4</sup>
Si	2.2 x 10 <sup>-3</sup>	S	5.33 x 10 <sup>-3</sup>
Ca	2.92 x 10 <sup>-3</sup>	Fe	7.32 x 10 <sup>-4</sup>

### 2.2.6.6 Shielding of the Final Focusing Magnets

Five superconducting quadrupoles are arranged along each beam line to focus the ion beam onto the target. Adequate shielding should be provided to protect the final focusing magnets from the streaming radiation. In a previous study,<sup>2,20</sup> it was shown that radiation effects in the magnets can be reduced significantly by tapering the inner surface of the shield along the direct line-of-sight of source neutrons in both the quadrupole and drift sections with all direct neutrons impinging on neutron dumps located in the drift sections between the quadrupoles. This results in increasing the minimum distance between the magnet and the point on the surface of the shield where the source neutrons have their first collision. It was shown that these modifications in the shield shape result in about three orders of magnitude reduction in peak magnet radiation effects compared to the traditional flat shield. A similar shield configuration is adopted to protect the final focusing magnets of Osiris.

The inner dimensions of the magnet shield along the beam lines were determined such that the shield does not interfere with the ion beams. The beam envelopes in the x and y directions have been utilized to determine the shield configuration. The shield is tapered along the direct line-of-sight of source neutrons generated in the target such that no direct source neutrons will impinge on the shield in the magnet sections. The shield configuration for the final focusing magnets is shown in Fig 2.16. The configuration is given for both the x and y directions. Notice that different scales are used for distances along the beam axis and in directions perpendicular to the beam axis. Three neutron dumps are utilized at distances of 25, 45, and 60 m from the target. Because of the relatively large beam envelope in the x direction, providing adequate shielding in this direction was given higher priority. A minimum shielding thickness of 0.3 m is maintained for the quadrupoles in this direction. In the y direction, the smaller beam envelope allows for thicker shield for the quadrupoles Q2, Q3, and Q4 as shown in Fig. 2.16. The inner bore radii and minimum shield thickness for the final focusing magnets are given in Table 2.12. Three-dimensional neutronics calculations have been performed for the HIBALL-II<sup>23</sup> final focusing magnets. A shield consisting of 63% 316 SS, 15% Pb, 17% B<sub>4</sub>C, and 5% H<sub>2</sub>O was used. 15 cm of this shield result in an order of magnitude radiation attenuation. Using the Osiris fusion power, magnet distances from target and minimum shield thicknesses, Table 2.13 gives the peak magnet radiation effects in the final focusing magnets of Osiris.

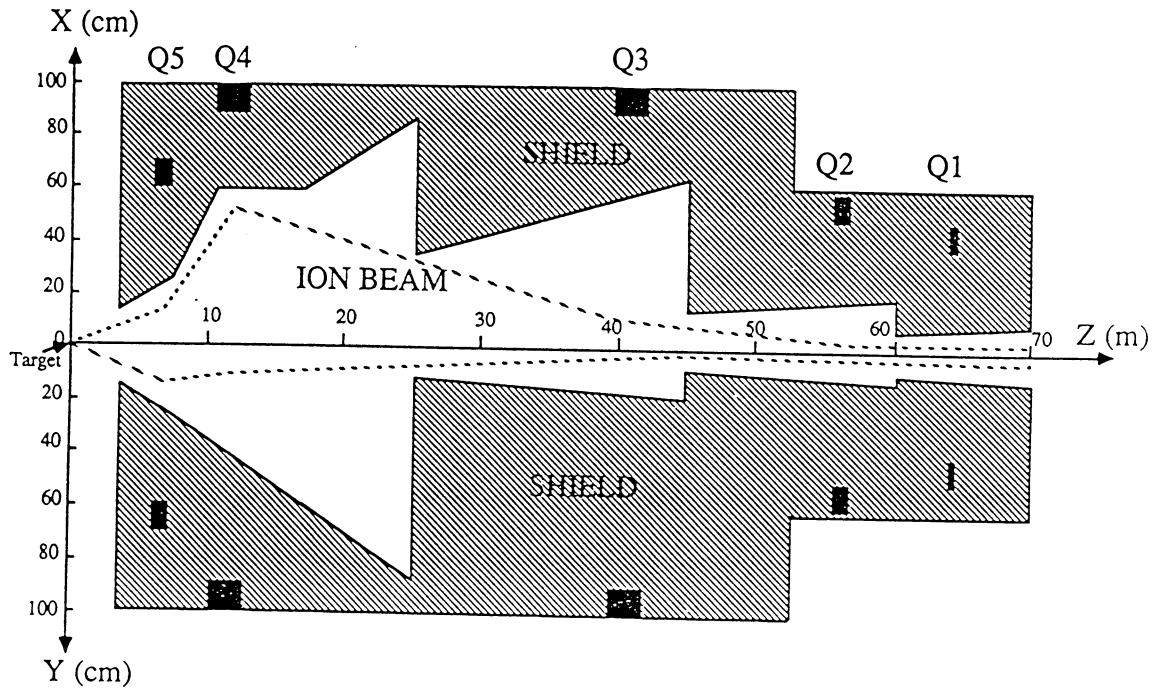


Fig. 2.16. Shield configuration for final focusing magnets of Osiris.

Table 2.12. Bore Radii and Shield Thicknesses for the Final Focusing Magnets

Magnet	Inner Bore Radius (m)	Minimum Shield Thickness in x Direction (m)	Minimum Shield Thickness in y Direction (m)
Q1	0.4	0.31	0.31
Q2	0.5	0.30	0.40
Q3	0.9	0.30	0.73
Q4	0.9	0.34	0.47
Q5	0.6	0.36	0.36

**Table 2.13. Peak Radiation Effects in the Final Focusing Magnets**

Magnet	Peak Cu dpa/FPY	Peak Magnet Power Density (mW/cm <sup>3</sup> )	Peak Insulator Dose (rads @ 30 FPY) <sup>a</sup>	Peak Fast Neutron Fluence (n/cm <sup>2</sup> @ 30 FPY) <sup>b</sup>
Q1	1.1 x 10 <sup>-7</sup>	7.2 x 10 <sup>-5</sup>	7.7 x 10 <sup>6</sup>	6.0 x 10 <sup>15</sup>
Q2	1.9 x 10 <sup>-7</sup>	1.2 x 10 <sup>-4</sup>	1.2 x 10 <sup>7</sup>	9.2 x 10 <sup>15</sup>
Q3	3.4 x 10 <sup>-7</sup>	2.0 x 10 <sup>-4</sup>	2.1 x 10 <sup>7</sup>	1.7 x 10 <sup>16</sup>
Q4	2.1 x 10 <sup>-6</sup>	1.2 x 10 <sup>-3</sup>	1.3 x 10 <sup>8</sup>	1.0 x 10 <sup>17</sup>
Q5	5.0 x 10 <sup>-6</sup>	2.9 x 10 <sup>-3</sup>	3.0 x 10 <sup>8</sup>	2.4 x 10 <sup>17</sup>

<sup>a</sup> Limit = 10<sup>9</sup> - 10<sup>10</sup> rads

<sup>b</sup> Limit = 10<sup>19</sup> n/cm<sup>2</sup>

The magnet radiation effects are the highest in the magnet closest to the target (Q5). The peak dpa rate in the copper stabilizer is only 5 x 10<sup>-6</sup> dpa/FPY implying that radiation induced resistivity at end-of-life (30 FPY) is only 0.1 nΩ-m.<sup>2,21</sup> Hence, magnet annealing is not required during the reactor lifetime.<sup>2,21</sup> Experimental results with 5 K irradiation of epoxy and polyamide insulators indicated that the insulator retains 75% of its mechanical strength with doses up to 10<sup>9</sup> and 10<sup>10</sup> rads, respectively.<sup>2,22</sup> The peak end-of-life insulator dose in Q5 is 3 x 10<sup>8</sup> rads implying that either epoxy or polyamide can be used for electric insulation. Currently available irradiation data indicate that end-of-life fast neutron fluences up to 10<sup>19</sup> n/cm<sup>2</sup> (E > 0.1 MeV) will not result in significant degradation in the Nb<sub>3</sub>Sn critical properties.<sup>2,23</sup> The results in Table 2.13 indicate that the peak fast neutron fluence levels in the magnets are well below the design limit. The peak winding pack nuclear heating is very small. The total nuclear heating in the five magnets along each beam line is estimated to be only about 1 W. Hence, the proposed magnet shield configuration will provide adequate protection for the final focusing magnets from streaming radiation.

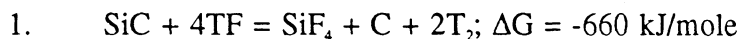
## 2.2.7 Tritium Recovery and Containment

### 2.2.7.1 Potential Chemical Reactions of Flibe

**Irradiated Liquid Flibe.** The fused salt system LiF-BeF<sub>2</sub> was extensively studied at ORNL for use in the Molten Salt Breeder Experiment<sup>2,24</sup> because of its low activation, high thermal stability, and low vapor pressure. The phase diagram indicates<sup>2,25</sup> a eutectic composition at 53 mole % BeF<sub>2</sub> and 364°C; however, because of the high BeF<sub>2</sub> content, this composition has an extremely high viscosity. The compound Li<sub>2</sub>BeF<sub>4</sub> (known as Flibe) melts at 459°C, has a lower viscosity, and was used in the experimental fission reactor studies to dissolve the fuel UF<sub>4</sub>.

The Molten Salt Breeder Experiment noted only light corrosion of the Ni-base alloys and graphite in contact with the molten salt containing fissionable UF<sub>4</sub>. The Flibe utilized Li7 so that tritium was produced only by the ternary fission of U-235 (1 atom/10,000 fissions). The neutronic reactions in an IFE reactor are different, however. An IFE breeder generates 1 atom T/fusion neutron by the nuclear reaction <sup>6</sup>Li(n,α)T with thermal neutrons forming copious amounts of TF, which may react with the metallic, SiC, or carbon (graphite) structures. The potential corrosion reactions were assessed by use of the thermodynamic free-energy<sup>2,25,2,26,2,27</sup> changes from reactants to products tabulated at 1000 K, as follows, based upon the use of HF data for TF.

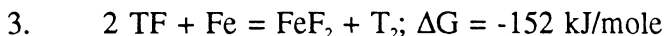
Potential reactions by TF:



This reaction is favored to go to completion.



This reaction is slightly unfavorable but could progress if gaseous T<sub>2</sub> and CF<sub>4</sub> were less soluble in the salt than TF and were removed in the off-gas system.

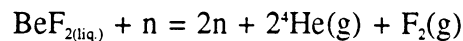


This reaction is favored to go to completion so that steel structures can not be used in the presence of TF. This reaction can be prevented by coating all the metallic structure with Mo or W. A technique was developed in which a Mo coating was formed in situ by dissolving a small amount of MoF<sub>6</sub> in the molten salt so that the MoF<sub>6</sub> was reduced as the Fe was oxidized to FeF<sub>2</sub>. The reaction continued until all the surfaces were covered

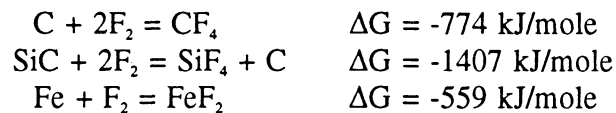
with Mo and could be repaired as needed. This technique, however, introduces FeF<sub>2</sub> and Mo into the salt phase, which results in the irradiation of Mo forming undesirable radioactive products. In addition, providing a Mo coating in the presence of carbon fibers, as utilized in Osiris, is not possible.

It would be very desirable to prevent the corrosion of steel components which may be used in the heat transfer system and SiC or carbon which could be used as first-wall materials. In order to prevent this corrosion, the compound TF in solution needs to be destroyed before it comes in contact with the structural materials. This can be accomplished easily by placing sacrificial Be spheres in the exit flow of the molten salt from the reactor. As was demonstrated for the MSBRE, the Be reduces all species in solution except LiF. The accumulating concentration of BeF<sub>2</sub> would be adjusted in a fuel clean-up side-stream in which new LiF will need to be added at its burn-up rate.

Another type of nuclear transformations with 14 MeV neutrons can cause further chemical corrosion of the structure. For instance, in an IFE reactor, neutrons above the 2.2 MeV threshold energy react with Be (which is unlikely in a fission reactor) by the nuclear reaction,



The free fluorine gas would react rapidly with SiC, carbon, or metallic structures to form the corresponding fluorides: SiF<sub>4</sub>, CF<sub>4</sub> and metallic fluorides, as shown by the following free-energy changes @ 1000 K.



This nuclear transformation would be enhanced closest to the first wall where the neutron energies are highest; consequently, the chemical attack would be greatest on the first wall materials.

**Flibe Decomposition by Target X-rays.** Potential chemical reactions may occur at an ablated first wall wetted with liquid Flibe. These reactions are caused by radiolytic products formed by the absorption of x-rays emitted from the burning target, which carry nearly 20% of the energy (~400 MW) at x-ray energies from 10 keV to 10 MeV. On the other hand, the chemical binding energy in the molecules of Flibe composition, 2 LiF + BeF<sub>2</sub>, is only 20 ev. As

a. result, many Flibe molecules completely decompose into their elementary atoms. The recombination of these atoms is difficult to predict without knowing the gaseous reaction rates at high temperature, but could lead to LiF, BeF, BeF<sub>2</sub>, LiBe and F<sub>2</sub>. The chemically reactive fluorine (F<sub>2</sub>) formed near the first wall would react rapidly with any first wall material (SiC, C, or metallic fibers).

In order to appraise the potential impact of the chemical, neutronic, and radiolytic decomposition products upon the first-wall materials (SiC or C), the potential corrosive effects of these materials were calculated for a full-power year (FPY). The following assumptions were made: (a) 50% of the TF formed from (LiF + n) reacted with the SiC first wall, but none with the C; (b) all the F atoms produced by the nuclear reactions with Be reacted with the first wall; and (c) the absorption of the x-ray energy in the ablated salt was based upon the following assumptions: a 5 mm thickness of Flibe covered the first wall, the attenuation factor of Flibe, which is mostly F atoms would be similar to oxygen, 5.57 cm<sup>2</sup>/g @ 10 keV x-rays,<sup>2,28</sup> and because the F atoms would react mostly with the vaporized salt atoms only 1% would react with the first wall.

The results of these preliminary calculations (Table 2.14) indicates that 8.5 mm thickness of SiC and 6.5 mm of C would be corroded per FPY. These calculations indicate that the useful lifetime of the first wall fabric could be < 1 FPY.

**Table 2.14. Potential Corrosion of First-Wall by Flibe Due to Nuclear Transformations and X-ray Decomposition**

Reactive Species	Carbon mm/yr	SiC mm/yr
TF <sup>(a)</sup>	-	0.5
F <sub>2</sub> <sup>(b)</sup>	0.9	1.4
F <sub>2</sub> <sup>(c)</sup>	<u>5.6</u>	<u>6.6</u>
Total	6.5	8.5

<sup>(a)</sup> Produced by neutronic absorption of <sup>6</sup>LiF and 50% of the TF reacts with the first-wall.

<sup>(b)</sup> Produced by neutronic absorption of BeF<sub>2</sub> and 100% reacts with the first-wall.

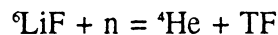
<sup>(c)</sup> Produced by x-ray decomposition of Flibe attenuated by 5 mm of Flibe and 1% of the F<sub>2</sub> reacts with the first wall.

The loss in the strength of these composites caused by the several corrosive effects noted will need to be experimentally determined because the corrosion may not be uniform, but may preferentially attack localized sites at high stress points, causing premature breakage of certain fibers without much overall corrosion. The following conclusions are drawn from the analysis of the potential chemical reactions in Flibe as used in the Osiris reactor.

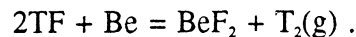
1. The first wall fabric should be composed of carbon fibers not SiC.
2. The tritium in the molten salt will be adjusted to exist as T<sub>2</sub> which can permeate through the IHX into the steam cycle.
3. Conservative estimates of the radiolytic decomposition of the Flibe near the first wall indicates that the corrosion of the carbon fibers may be 6.5 mm/FPY. The loss in the strength of the fabric due to this corrosion needs to be evaluated.

#### 2.2.7.2 Tritium Recovery

**Chemical Form of Tritium.** The neutron irradiation of Flibe causes the following nuclear reaction,



Consequently, the reactive chemical species TF accumulates in the salt and, as previously noted can corrode SiC or a steel structure. It is desirable, therefore, to reduce TF by use of the chemical reaction,



Both the BeF<sub>2</sub> and the T<sub>2</sub> remain dissolved in the fused salt. It is desirable to reduce the TF as soon as it is formed; consequently, a bed of Be spherical particles is embedded at the bottom of the pool in the Osiris reactor chamber, because all the salt in the chamber must exit through this pool. The total flow of salt from the pool is 7000 kg/s, ~3.5 m<sup>3</sup>/s, while the tritium addition is at the rate of 12.1 x 10<sup>-3</sup> g T/s; consequently, the T<sub>2</sub> concentration is 5.8 x 10<sup>-4</sup> moles T<sub>2</sub>/m<sup>3</sup> (salt) or 1.7 x 10<sup>-3</sup> wtppm.

The solubility of T<sub>2</sub> in the molten Flibe can be expressed by the Henry's Law constant,<sup>2,25</sup> K<sub>H</sub>, obtained from measurements with H<sub>2</sub>, i.e.

$$K_H = \frac{7 \times 10^{-7} \text{ moles } T_2}{m^3 (\text{salt}) \text{ Pa}},$$

at 1000 K. Based upon this relationship and the value of the T<sub>2</sub> concentration in the salt, we

calculate a  $T_2$  pressure of 820 Pa. At such a high pressure  $T_2$  gas would permeate easily through the IHX and be lost to the environment. It is necessary, therefore, to reduce the  $T_2$  concentration in the salt before it reaches the IHX to a level so that the tritium permeation rate is acceptable.

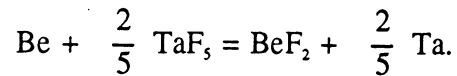
Tritium is removed from Flibe as it cascades down the back of the blanket and is then pumped out by the chamber vacuum systems. If the tritium concentration is not reduced enough by the cascade, a vacuum disengager will be needed.

**Design of the Vacuum Disengager.** In order to remove rapidly a dissolved gas from a liquid, it is necessary to create a large liquid to gas surface area. Recently, Dolan et al.,<sup>2,29</sup> have designed a vacuum disengager to remove  $T_2$  from Flibe in HYLIFE-II. This disengager consists of a spray of 400  $\mu\text{m}$  droplets of molten salt falling vertically downward at a height of 5 m while in a vacuum chamber. The pumping capacity of the vacuum chamber is sufficient to obtain a decontamination factor of  $10^5$  for a 2-stage system so that the  $T_2$  concentration dissolved in the salt at the exit from the disengager is  $5.8 \times 10^{-9}$  moles  $T_2/\text{m}^3$ . An orifice plate where the droplets are formed is 4.2 m dia. ( $13.9 \text{ m}^2$ ) for a flow rate of 6.3 in HYLIFE-II, while for Osiris with a flow rate of 3.5  $\text{m}^3/\text{s}$ , this plate would be only 3.2 m dia.

The vacuum disengager for Osiris would consist of two evacuated right-circular chamber, 3.2m dia. x 5 m high, with 10% of the orifice plate area containing holes for the formation of the droplets. These chambers must be well-insulated because all of the heat transfer fluid transits these chambers before the IHX.

**Removal of Target Debris.** In addition to unburned DT in the target debris, other constituents are the tamper materials, either Pb or Ta, and the ablator material, probably a polymer of  $(\text{CH}_2)_n$  or  $(\text{CD}_2)_n$ . All these materials will be vaporized by the target explosion and become mixed with the Flibe vapors ablating from the first wall. The recombined carbon-hydrogen species will probably form methane, perhaps containing some fluorine; consequently, the methane should remain as a gas and exit from the reactor chamber via the vacuum system. The metals, Pb and Ta, would form their corresponding fluorides,  $\text{PbF}_2$  and  $\text{TaF}_5$ , which would remain dissolved in the Flibe. Because both Pb and Ta form undesirable radioactive products upon neutron irradiation, it is necessary to control the quantities of these debris products in the Flibe.

Both  $\text{PbF}_2$  and  $\text{TaF}_5$  will react with the Be balls at the bottom of the reactor pool. For instance, the reaction with Ta is



Based upon the free-energy of formation of these compounds at 900 K, it has been shown<sup>2,30</sup> that the concentration of  $\text{TaF}_5$  in the system should be,

$$\text{Conc. TaF}_5 = \frac{0.254 \text{ ppm} \cdot \text{moles (TaF}_5)}{\text{mole (BeF}_2)}$$

One mole of  $\text{BeF}_2$  exists in one mole of  $\text{Li}_2\text{BeF}_4$  with a molecular wt of 99 g/mole, and one g-atom of Ta at 181 g/g-atom, so that the concentration of Ta in the Flibe would be 0.46 wtppm. Caution should be used in assessing this value because it assumes ideal thermodynamic efficiency and it also assumes that the reduced metallic Ta can be quantitatively removed from the salt. This separation may be difficult at such a small concentration because the Ta may form a colloidal suspension and be difficult to filter from the salt and may require special treatments, which need to be developed. A more reasonable value would be 1 wtppm (Ta) in the Flibe. Based upon this value and the total Flibe in the system, 940 Mg, the total Ta in the system would be 940 g(Ta). Also, all the Flibe flowing through the vacuum disengager should initially pass through the Ta separation device, or the colloidal Ta might interfere with the formation of the small droplets in the disengager.

**Estimate of Tritium Permeation.** The permeation of tritium at the IHX could represent a path for significant tritium release to the environment. The tritium concentration in the Flibe entering the IHX is  $5.8 \times 10^{-9}$  moles  $\text{T}_2/\text{m}^3$  (salt) and based upon the Henry's law constant, a partial pressure of  $8 \times 10^{-3}$  Pa of  $\text{T}_2$  supplies the driving force for permeation through the IHX tubes. The usual method to calculate this permeation has been to use the permeation constant for  $\text{T}_2$  in the metallic tubes times the  $(P_{\text{T}_2})^{1/2}$ . Such a calculation is based upon the assumption that the tritium concentration is a constant value at the Flibe/tube interface which can be calculated from  $(P_{\text{T}_2})$ . Longhurst and Dolan<sup>2,31</sup> have analyzed these assumptions and determined that for Flibe solutions containing (T), the tritium near the salt/tube interface quickly becomes depleted due to permeation through the tube, and the diffusion of  $\text{T}_2$  to this surface layer is slow,

becoming the rate determining step. Based upon these assumptions, they determined that the total tritium permeation through the IHX was 7.3% of the total tritium per day which flows through the IHX for the HYLIFE-II system which is similar to that required for Osiris. Their results indicated that the tritium permeation increased slightly with the concentration of  $T_2$  and increased directly with the length of the IHX tubes (e.g., surface area for the same dia. tubing). These results are directly scalable to Osiris, in which the Flibe flows through the disengager and subsequently carries 105 Ci/d of  $T_2$  through the IHX. The amount of  $T_2$  which permeates is 7.3% of this value times the length of tubes (surface area) of the Osiris IHX which is 4 times that of HYLIFE-II model.<sup>2.31</sup> Based upon these assumptions, the calculated permeation for Osiris would be 30 Ci/d of  $T_2$ . The total inventory of tritium in the Flibe is based upon the total inventory of ~470 m<sup>3</sup> (salt) in the reactor chamber and the heat transfer system. Approximately half of this total volume would be at the concentration existing at the exit from the reactor and half at the concentration subsequent to the disengager, giving a total inventory of ~1 g(T) for the entire Flibe system.

### **2.2.7.3 Tritium Inventory and Potential Loss Rate**

In order to determine the steady-state and accidental tritium releases from the plant-site the tritium inventories and locations throughout the plant were assessed as shown in Table 2.15. Osiris has a fusion power of ~2000 MW and, therefore, must burn a ~300g of tritium per day. Assuming a typical burn fraction of 30%, ~1000 g of tritium must be injected each day since the tritium breeding ratio is 1.24, 1070 g of tritium must be recovered daily. The routine tritium releases were, then, based upon the daily flow rate of tritium through each piece of apparatus, based upon the TSTA experience<sup>2.32</sup> that ~1 Ci/d of tritium is released per 100 g of tritium processed in well-enclosed secondary containment systems.

**Table 2.15. Tritium Locations, Inventories, Flow Rates, and Potential Release Rates**

Location	Inventory g(T)	Flow Rate g/d	Routine Ci/d	Accidental g(T)
Reactor System				
Breeder	1	~1070	10	1
Graphite	4	-	-	2 (50%)
Steam generator to coolant water	-	-	30	-
Beam line	1	10	1	1
Containment Building				
Atmosphere	~0	-	-	-
Fuel Injector	1.2	~1000	10	1.2
Fuel Reprocessing				
Vacuum disengager	44	~1070	10	-
Cryo-distillation	9.5	~1070	10	-
Target factory	260	~1000	10	100

**The Reactor and Heat Transfer System.** This system consists of the total Flibe in the reactor, the vacuum disengager, the IHX and the connecting pipes for a total of 470 m<sup>3</sup> (940,000 kg). Approximately 50% of this molten salt, mostly in the reactor and vacuum disengager, is at a concentration of  $5.8 \times 10^{-4}$  moles (T<sub>2</sub>)/m<sup>3</sup> while the other 50% is at a concentration of  $\sim 10^{-8}$  moles (T<sub>2</sub>)/m<sup>3</sup>; consequently, the total tritium inventory in Flibe is  $\sim 1$  g(T). In a severe accident, perhaps only 50% of the gaseous tritium would be released before the salt solidifies, because there is no major radioactive nuclides in this salt to prolong its heating. Based upon the flow rate of tritium in the breeder of 1070 g/d, a well-enclosed system would off-gas  $\sim 10$  Ci/d.

The graphite fibers forming the first-wall ( $\sim 3000$  kg) are subjected to a T<sub>2</sub> pressure from the tritium dissolved in the Flibe and, also, subjected to the ion flux from the target debris. Under such circumstances, it has been observed that the H(T) atoms saturate along the grain-

boundaries at 5 atomic ppm T/C; consequently, the maximum tritium inventory in these fibers would be 4 g(T). The c/c composite forming the tank is subjected to only a low  $T_2$  pressure; consequently, it absorbs  $<0.1$  g(T).

The loss of tritium through the heavy-ion beam port could become a serious contamination in the accelerator facility unless it is well-managed. There are two sources of tritium which could enter the beam port: namely, (1) the continual evaporation of TF from the Flibe and (2) the unburned target fuel which is propelled throughout the chamber following each target ignition. These two sources were evaluated as follows:

**Evaporation of TF from the Flibe.** The unburned target fuel represents a tritium source of  $8.2 \times 10^{-3}$  g(T)/s; consequently, at the radial distance to the entrance of the beam port from the target, 5.5 m, the (T) flux is only  $2.2 \times 10^{-5}$  g(T)/m<sup>2</sup>·s. For beam port entrance area of 1.4 m<sup>2</sup>, ~10 g(T)/day effuses into the beam port; as a result, cryogenic adsorption traps must be installed along the internal surface of the beam tube. In addition, other vapors in the chamber, such as gaseous TF with a freezing point of 190 K and vaporized Flibe which solidifies at 732 K, will be swept into the beam ports. The cryo-fluid for the absorber plates could be liquid nitrogen at 77 K. These absorber traps could be placed along the flat surfaces constructed as neutron absorbers in the beam port nozzle. Two cryo-absorber plates would be installed back-to-back at each location selected so that one trap would be in use while the duplicate trap would be heated to evaporate the absorbed gases.

Some gases, such as DT, would not be absorbed on the nitrogen-cooled traps and would continue deeper into the beam tube, plus the vapors which are directly in-line with the center of the beam line. Both of these species would impinge upon the inner surface of the beam-line at the point where it begins to bend. At this bend and at locations deep into this bend, large cryo-adsorber surfaces would be installed using liquid He coolant which would adsorb the species DT and  $T_2$  which solidify at ~20 K. All of these traps would accumulate the 10 g(T)/d. If they are recycled every two hours, their total inventory is only 1 g(T). If the adsorption and degassing of these absorbers are tightly controlled to prevent leakage, then the loss of tritium further into the beam facility would be much less than 1 Ci/d. Nearly all of this tritium would be deposited in the vacuum pumps installed along the beam line.

**Tritium in the Containment Building.** The containment building would contain the Osiris reactor and perhaps the vacuum disengager and the IHX. Because each of these systems

contains tritium at high temperature, the possibility of tritium loss by permeation or leakage exists; consequently, all these systems and connecting pipes would be within secondary enclosures. As a result, the atmosphere in the building should contain very little tritium or other radioactive gases.

The target delivery system located near the reactor contains tritium; however, the number of targets on hand is limited to ~1 min fueling time so that the quantity of tritium is only 1.2 g(T) which could be released in an accident. The target delivery system handles 1000 g(T)/d, which is projected to release ~10 Ci/d for a well-enclosed apparatus.

**Fuel Reprocessing Facility.** High tritium inventories exist in the fuel processing facility principally in two systems: namely, (1) the vacuum pumps from the vacuum disengager and (2) the cryo-distillation system. The vacuum disengager must separate T<sub>2</sub> from the molten Flibe at the rate which it exits the reactor chamber by the use of vacuum pumps capable of maintaining low pressures. Such pumps could be turbo-molecular or cryo-absorption pumps. Because of the possibility of Flibe vapors and TF contamination in the gas stream, cryo-absorption pumps are suggested. If these pumps are on stream for one-hour, their inventory would be 44 g(T). Such pumps would process 1070 g(T)/d and with secondary enclosures would be expected to release only 10 Ci/d of tritium. Most of the tritium from the cryo-absorption pump should be DT which would go directly to the distillation system. The cryo-distillation system must handle 1070 g(T)/d. Based upon the design of an advanced distillation system,<sup>2,33</sup> the constant inventory of tritium in the distillation system would be 9.5 g(T) and the loss of tritium would be ~10 Ci/d. Both the cryo-absorption pumps and the cryo-distillation systems operate at sub-atmospheric pressures. If such systems are accidentally heated and evaporate the cryogenic fluids, then a passive safety seal is ruptured and the tritium contents of the equipment is vented to a large, preexisting, evacuated tank; consequently, no accidental release of tritium is predicted.

**Target Factory.** The target factory must fill ~400,000 targets/d with a total of 1000 g(T). For well-enclosed processing apparatus, the total tritium loss out the stack is expected to be 10 Ci/d. The rate of target filling is maintained at the rate of usage so that no large quantities of tritium in targets are in storage. The total inventory along the production line is limited to 260 g(T); however, 160 g(T) is enclosed in two liquid cryogenic containers, surrounded by evacuated chambers. These chambers are connected to evacuated tanks; consequently, if the apparatus becomes overly pressurized, a passive seal breaks and vents the tritium to the tank

which has sufficient capacity to contain all the  $T_2$  at a low pressure. The tank may also contain a tritium getter to immobilize the  $T_2$ . Because of this fail-safe system, the maximum  $T_2$  release would be only 100 g(T) in auxiliary components.